Supporting Information

1. Supplementary Figures

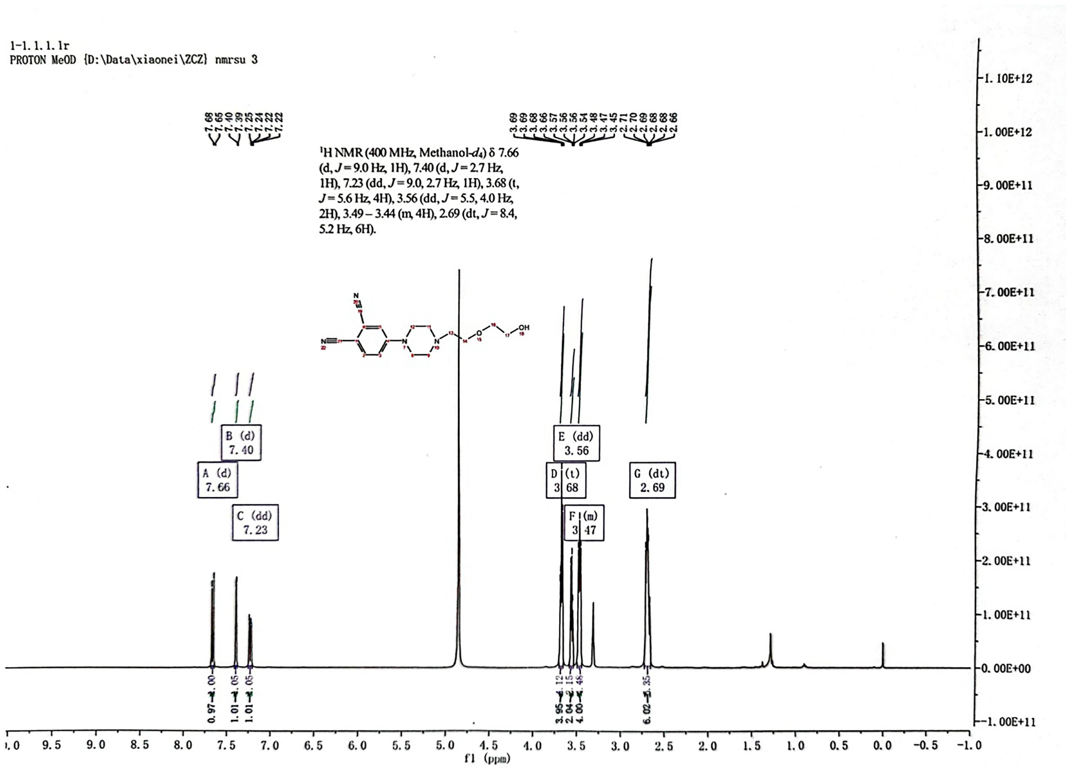

Figure S1. ¹H-NMR spectrum of intermediate 2 in MeOH.

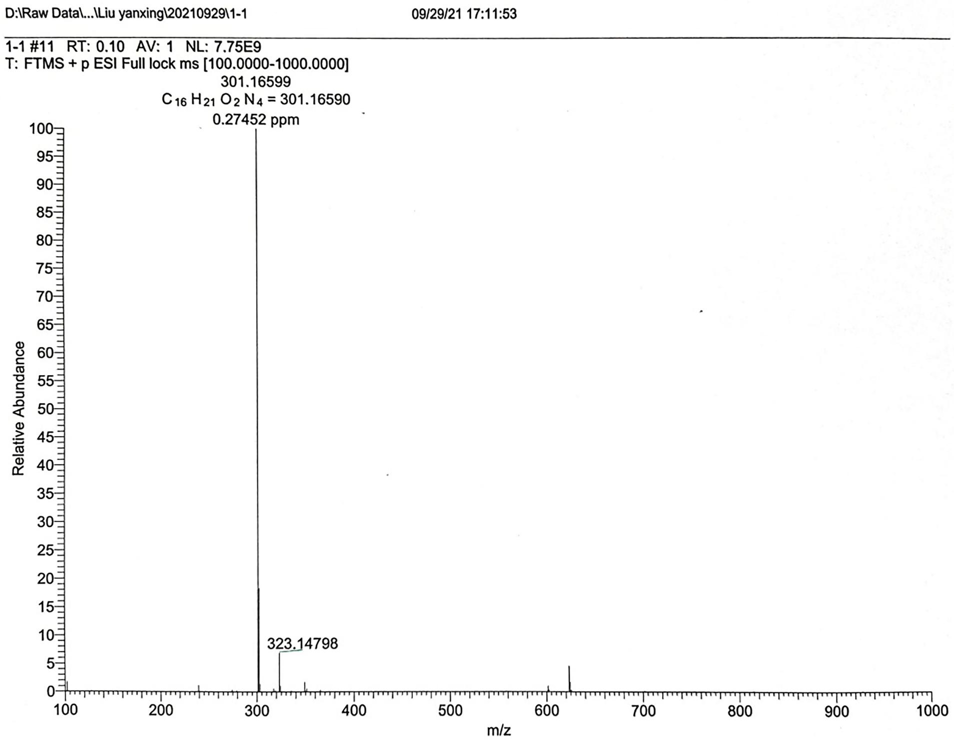

Figure S2. HRMS of intermediate 2.

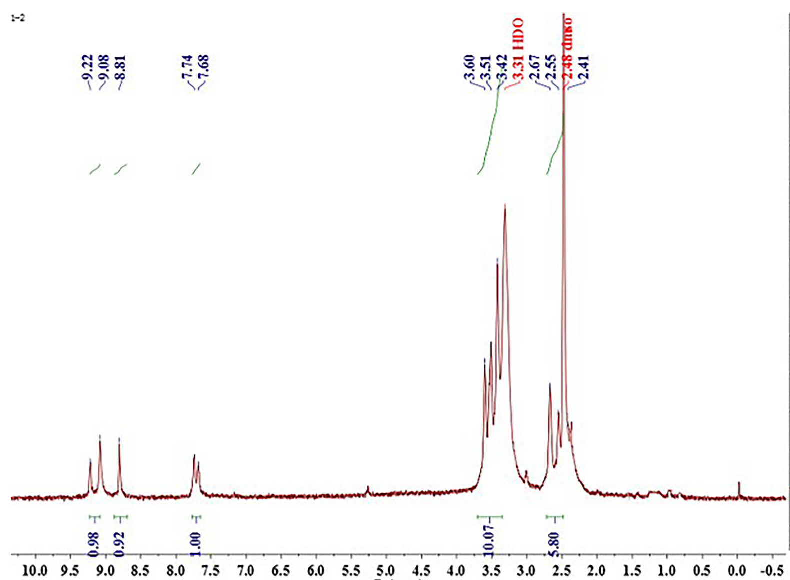

Figure S3. ^{1}H-NMR spectrum of ZnPc 1 in DMSO.

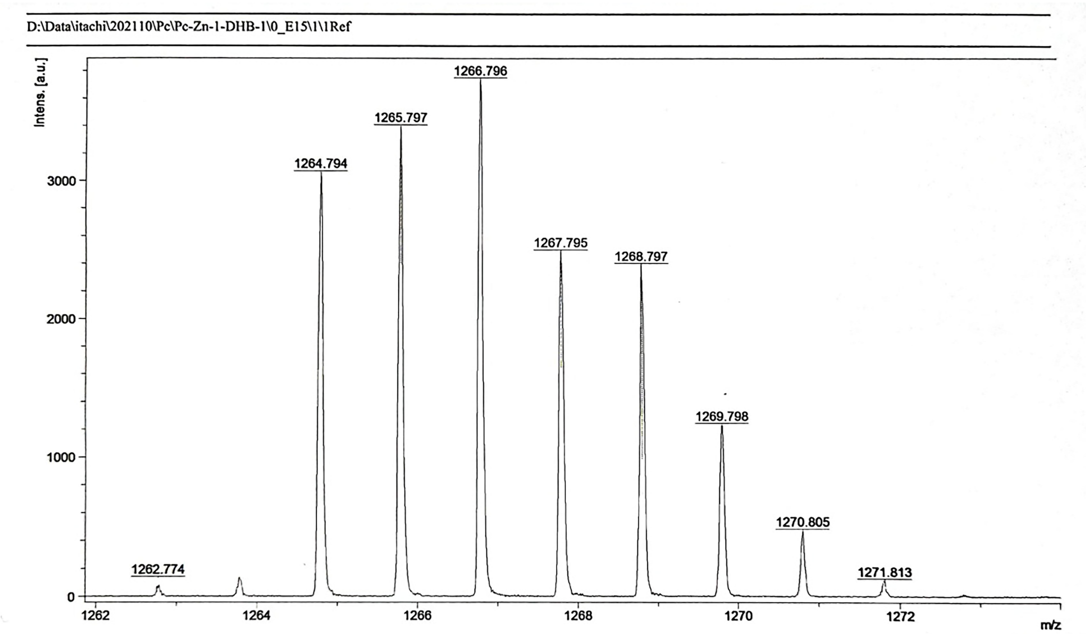

Figure S4. MALDI-TOF-MS of ZnPc 1.

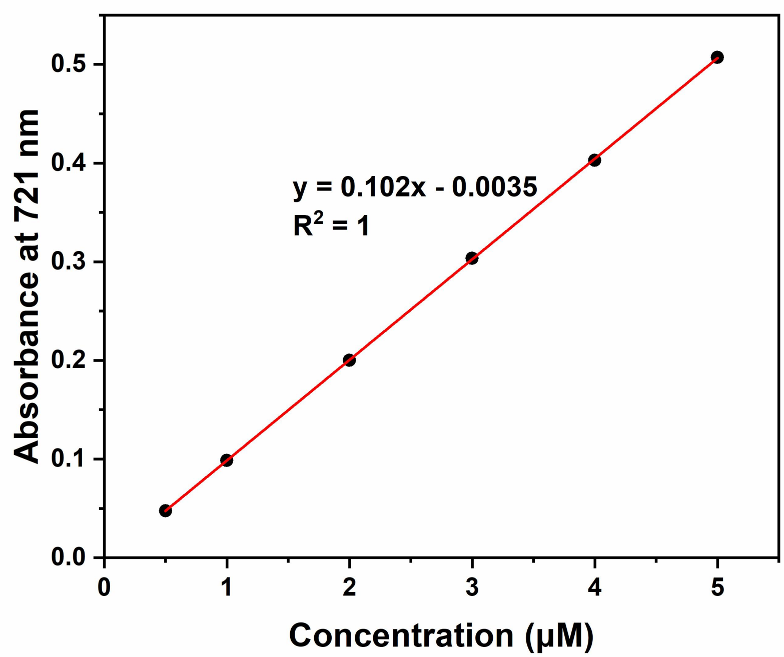

Figure S5. The liner plot of the absorbance of ZnPc 1 in DMSO in the Q-band (λ_{max}) as a function of concentration.

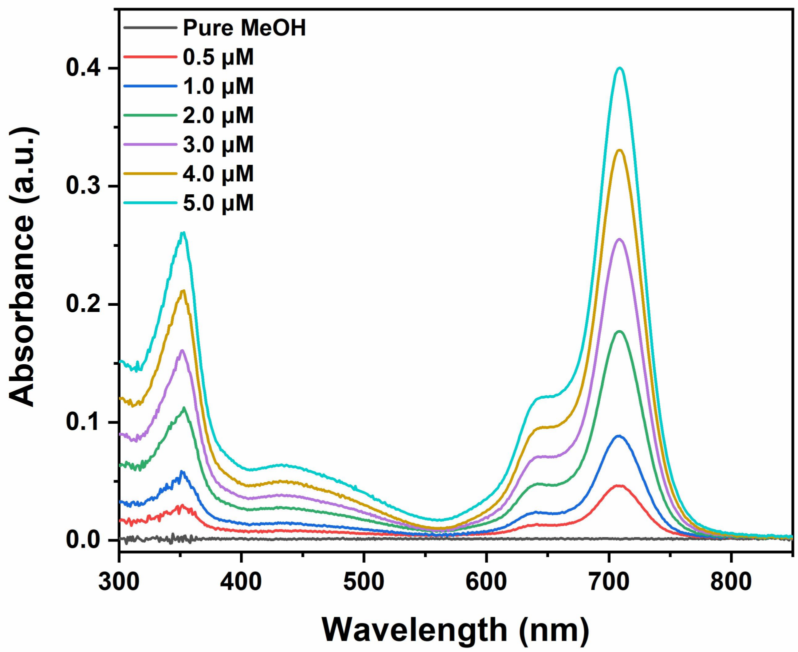

Figure S6. UV–Vis absorption spectra of ZnPc 1 in MeOH.

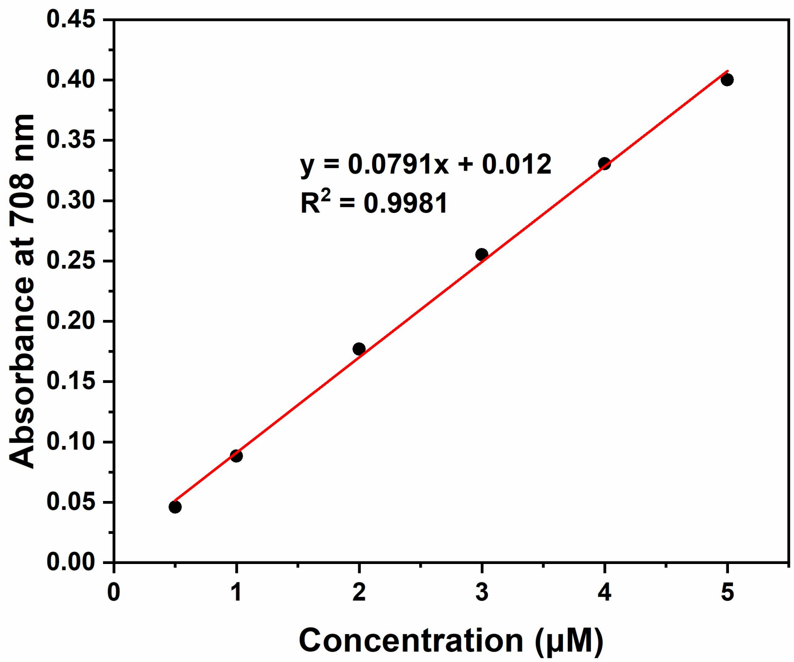

Figure S7. The liner plot of the absorbance of ZnPc 1 in MeOH in the Q-band (λ_{max}) as a function of concentration.

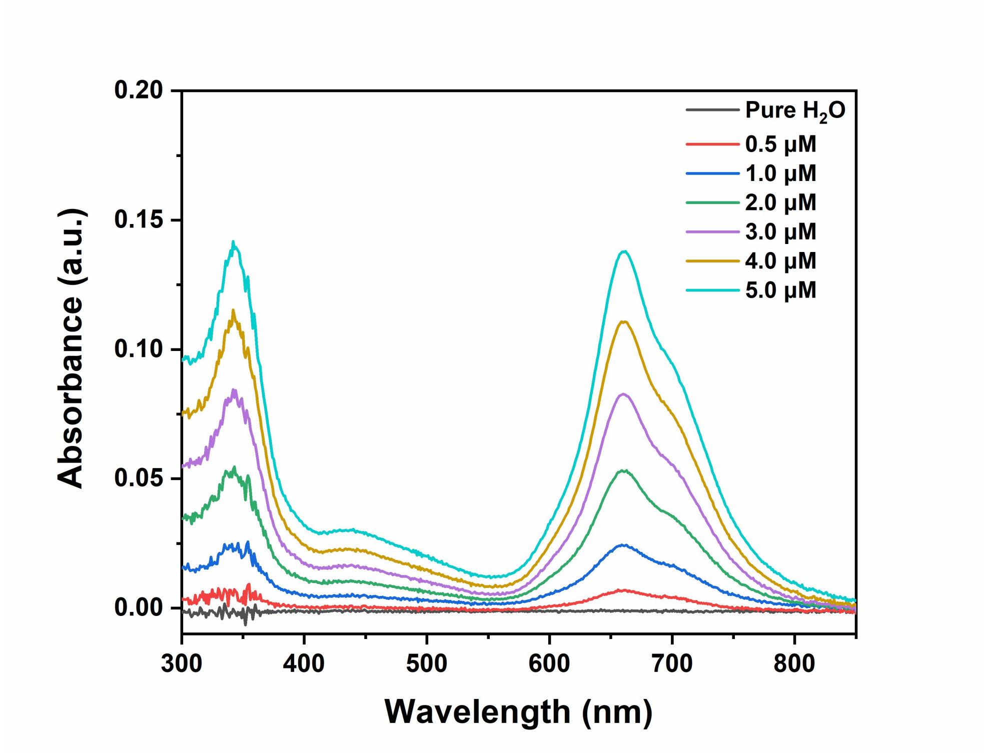

Figure S8. UV–Vis absorption spectra of ZnPc 1 in water.

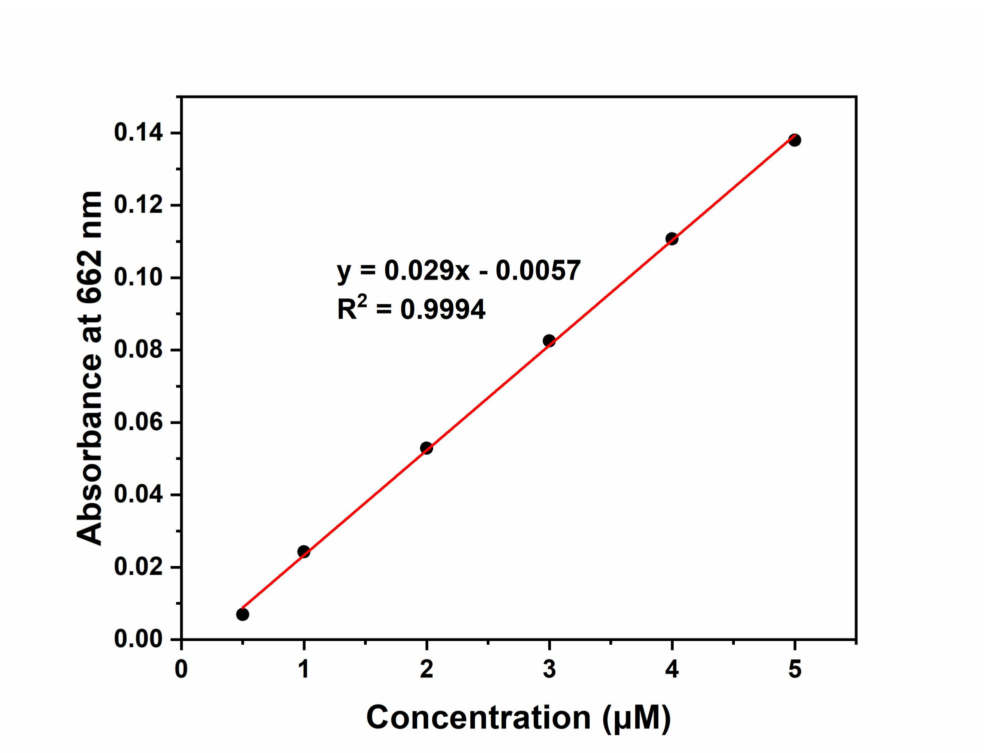

Figure S9. The liner plot of the absorbance of ZnPc 1 in water in the Q-band (λ_{max}) as a function of concentration.

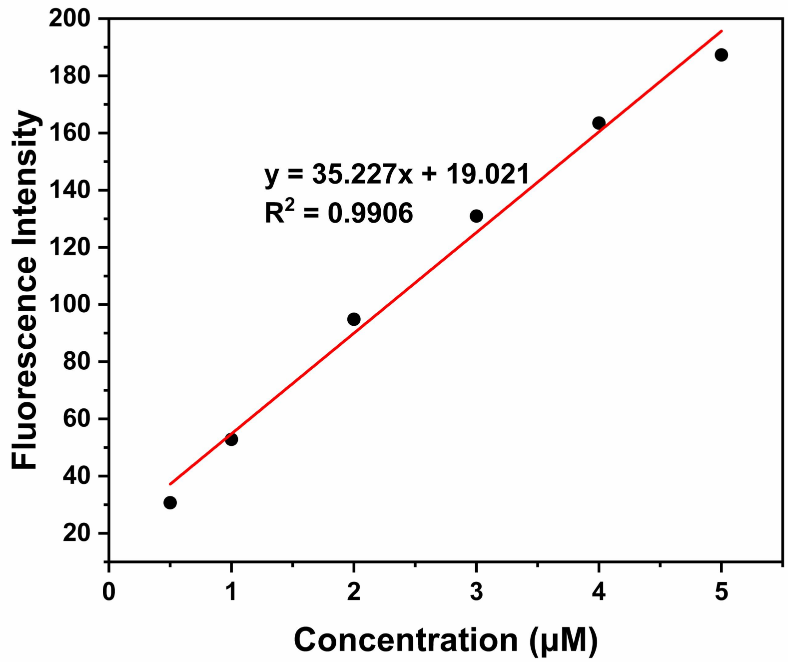

Figure S10. The line graph of the FL intensity of ZnPc 1 with λ Ex = 649 nm as a function of concentration in DMSO.

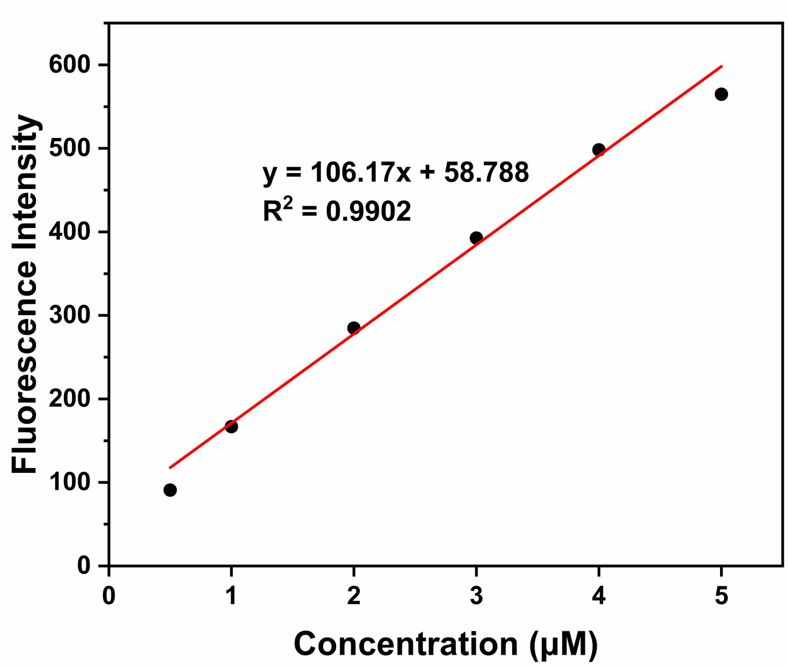

Figure S11. The line graph of the FL intensity of ZnPc 1 with λ Ex = 700 nm as a function of concentration in DMSO.

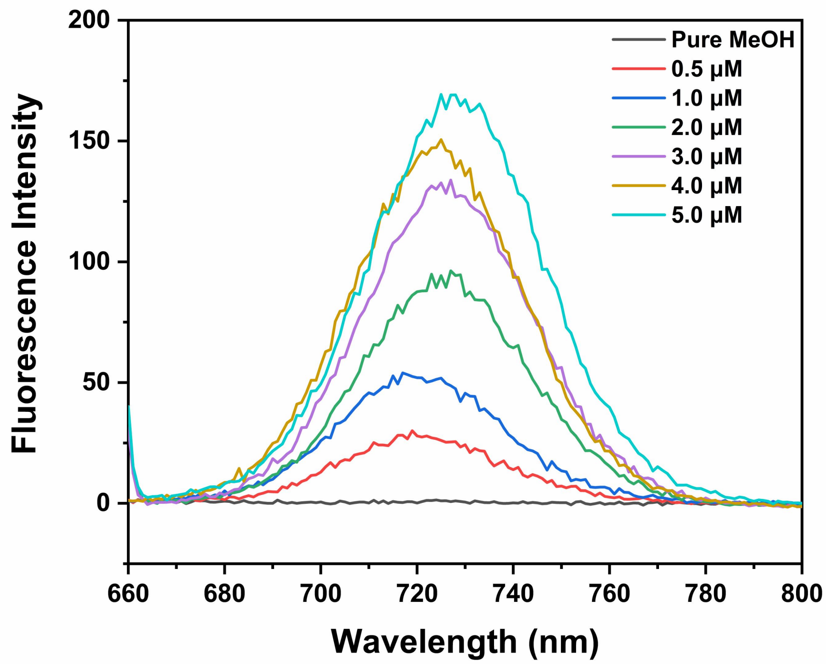

Figure S12. FL emission spectra of ZnPc 1 in MeOH with λ_{Ex} = 649 nm.

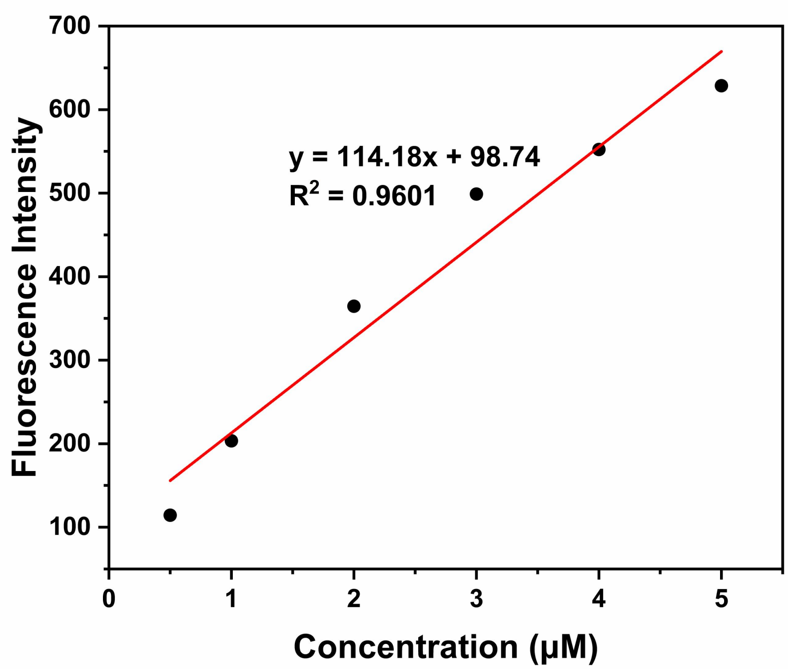

Figure S13. The line graph of the FL intensity of ZnPc 1 with λ_{Ex} = 649 nm as a function of concentration in MeOH.

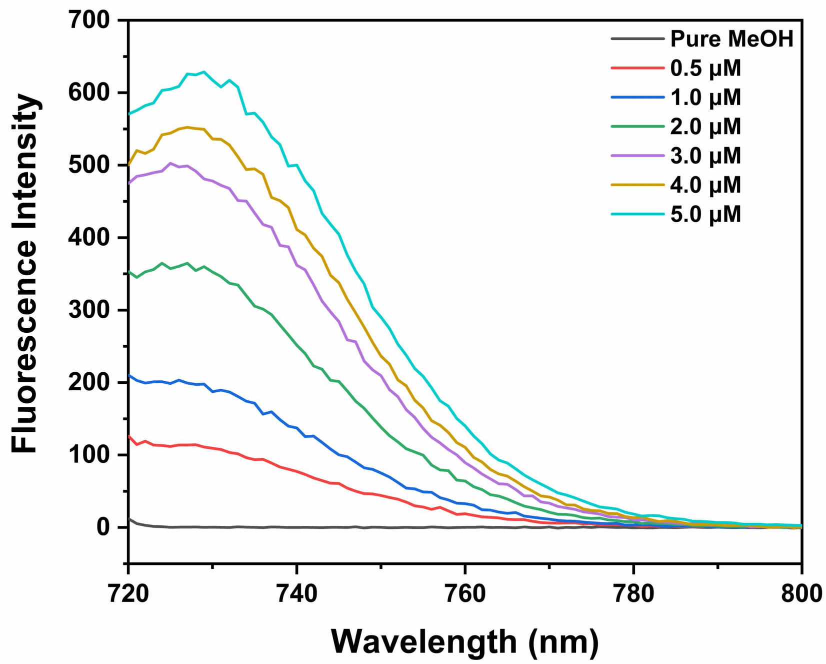

Figure S14. FL emission spectra of ZnPc 1 in MeOH with λ_{Ex} = 700 nm.

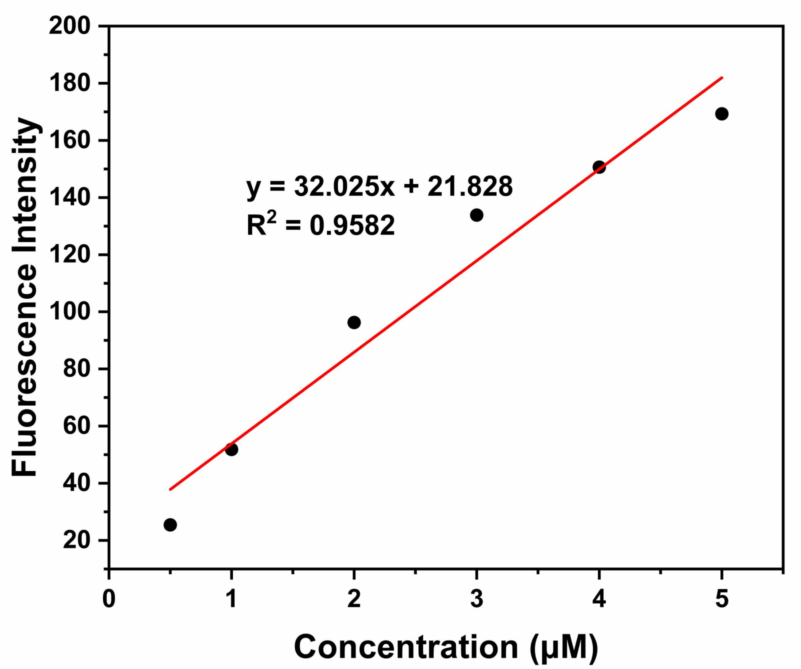

Figure S15. The line graph of the FL intensity of ZnPc 1 with λ_{Ex} = 700 nm as a function of concentration in MeOH.

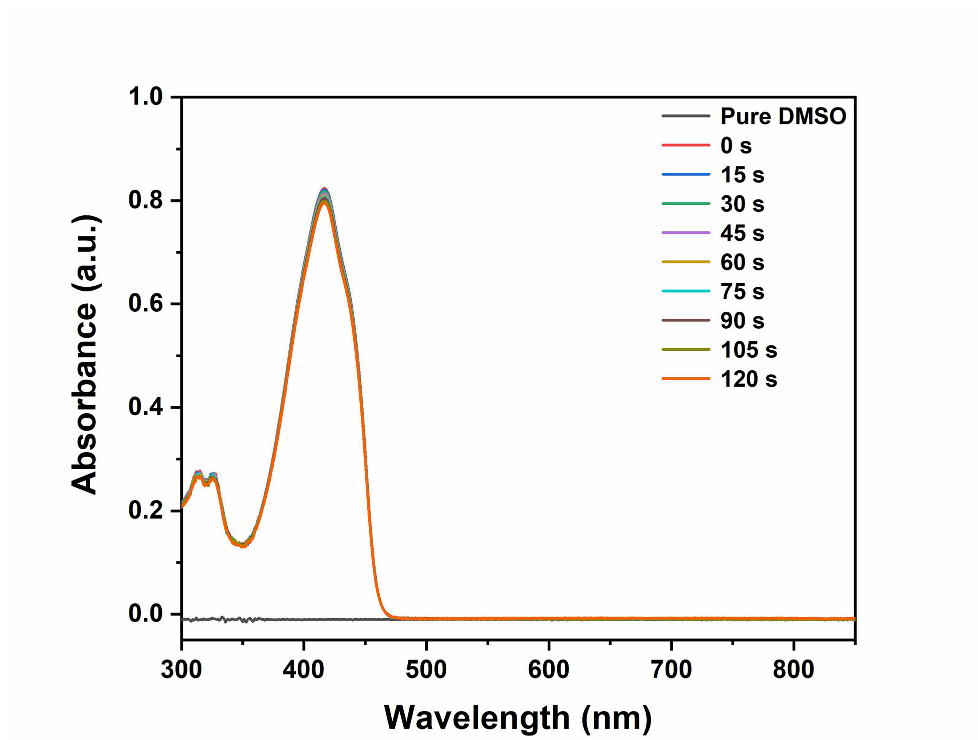

Figure S16. The UV−Vis spectra of DPBF in DMSO for different irradiation times under 690 nm laser irradiation (0.2 W/cm^2).

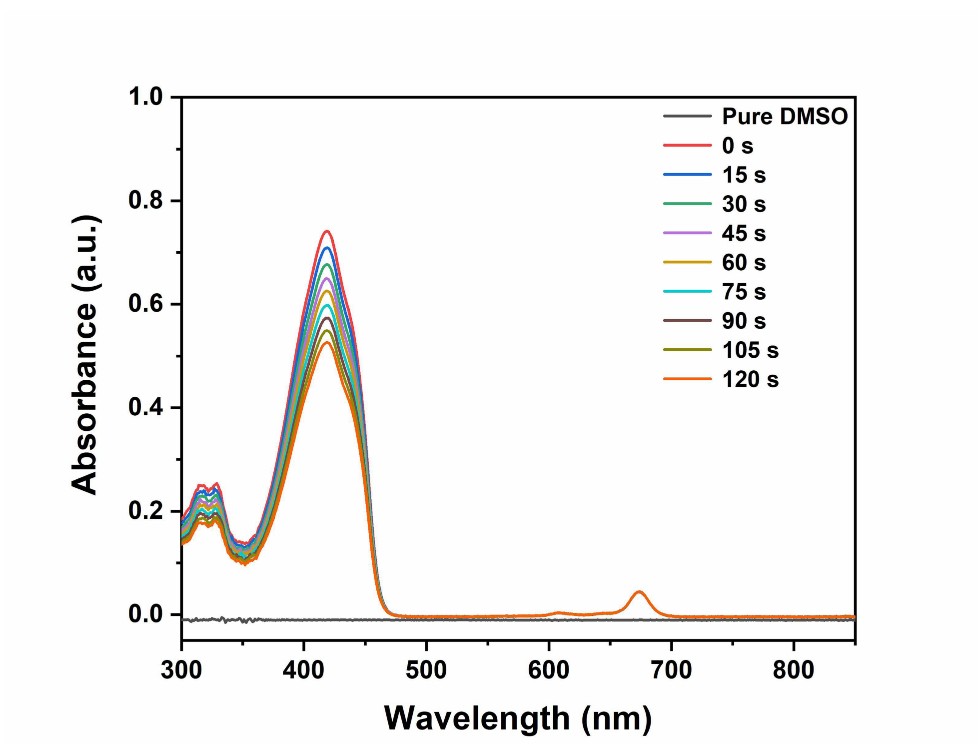

Figure S17. The UV–Vis spectra of DPBF containing ZnPc in DMSO for different irradiation times under the 690 nm laser irradiation (0.2 W/cm^2).

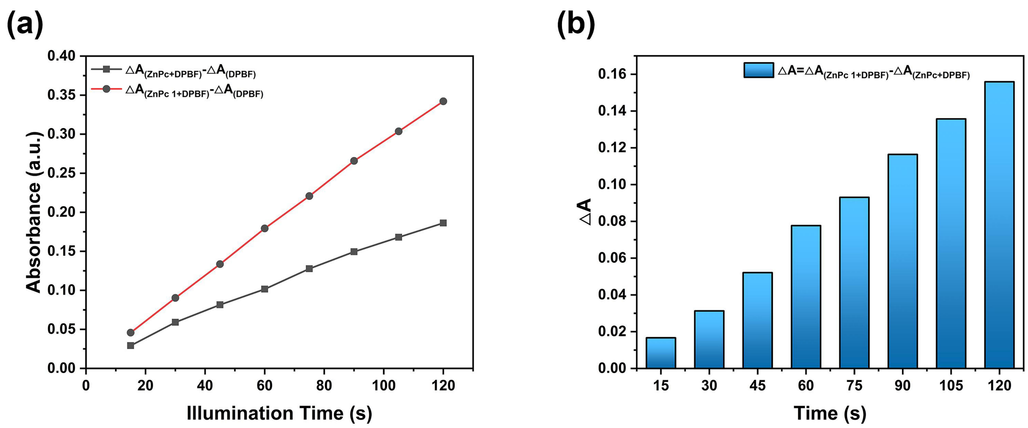

Figure S18. (a) The corresponding relative absorbance variations of different groups ($\triangle A_{(ZnPc+DPBF)}$-$\triangle A_{(DPBF)}$ and $\triangle A_{(ZnPc\ 1+DPBF)}$-$\triangle A_{(DPBF)}$) at different irradiation times under the 690 nm laser irradiation (0.2 W/cm^2). (b) The corresponding relative Increased absorbance variations of ZnPc 1 at different irradiation times under the 690 nm laser irradiation (0.2 W/cm^2).

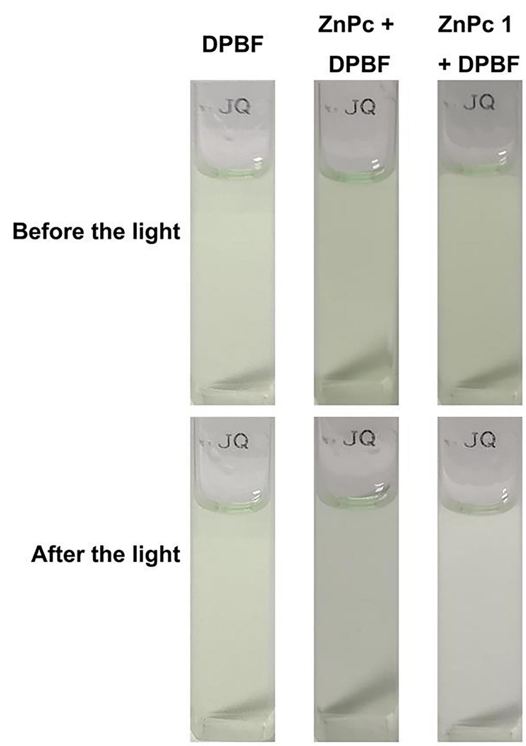

Figure S19. Comparison of DPBF degradation before and after 690 nm laser irradiation (0.2 W/cm^2, 2 min).

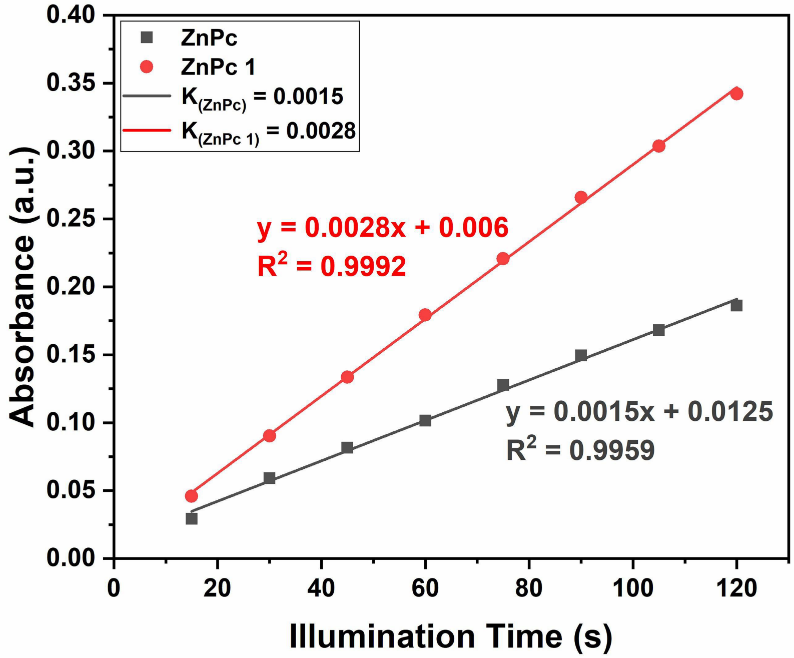

Figure S20. The linear diagram of difference in absorbance of ZnPc or ZnPc 1 at 415 nm as a function of illumination time.

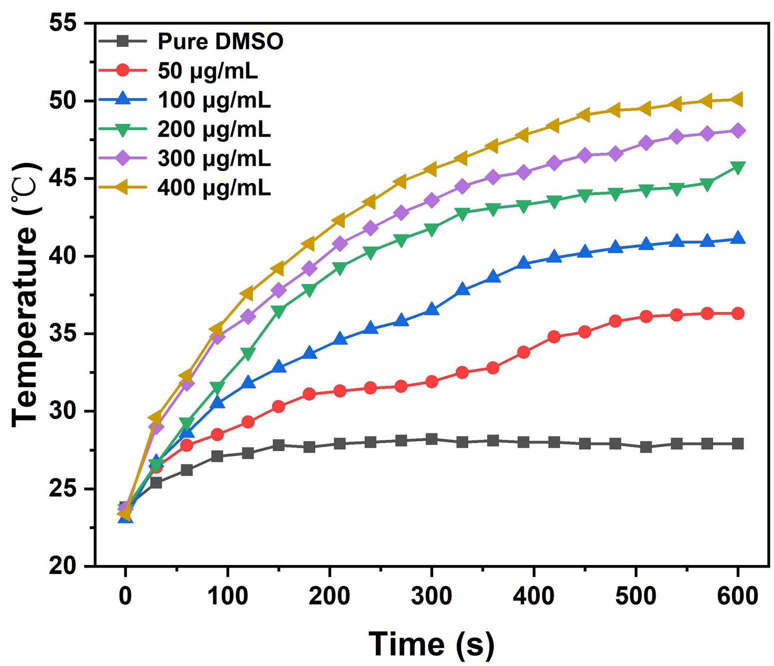

Figure S21. Temperature elevation of ZnPc 1 in DMSO in dependence of concentration (808 nm, 1.75 W/cm^2).

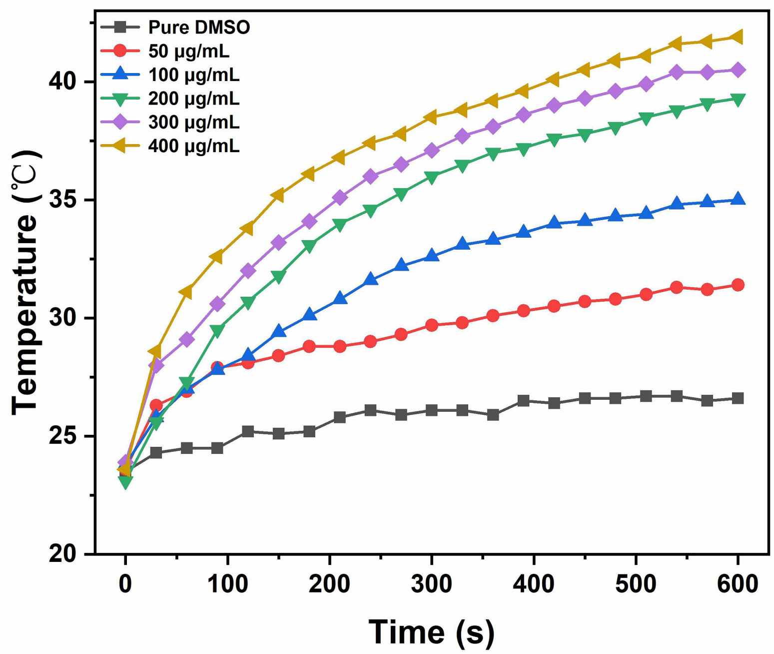

Figure S22. Temperature elevation of ZnPc 1 in DMSO in dependence of concentration (808 nm, 1.0 W/cm^2).

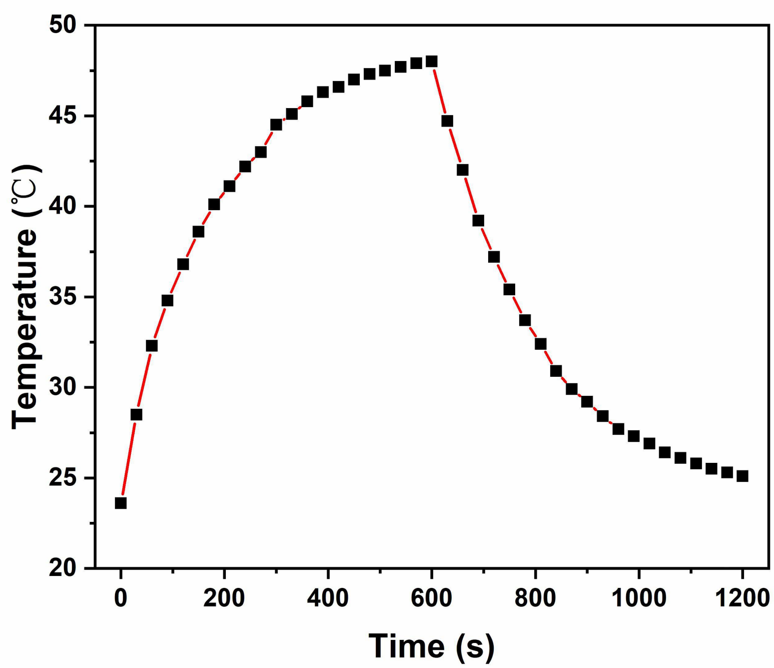

Figure S23. Photothermal effect of ZnPc 1 in DMSO irradiated with 808 nm laser (1.75 W/cm^2).

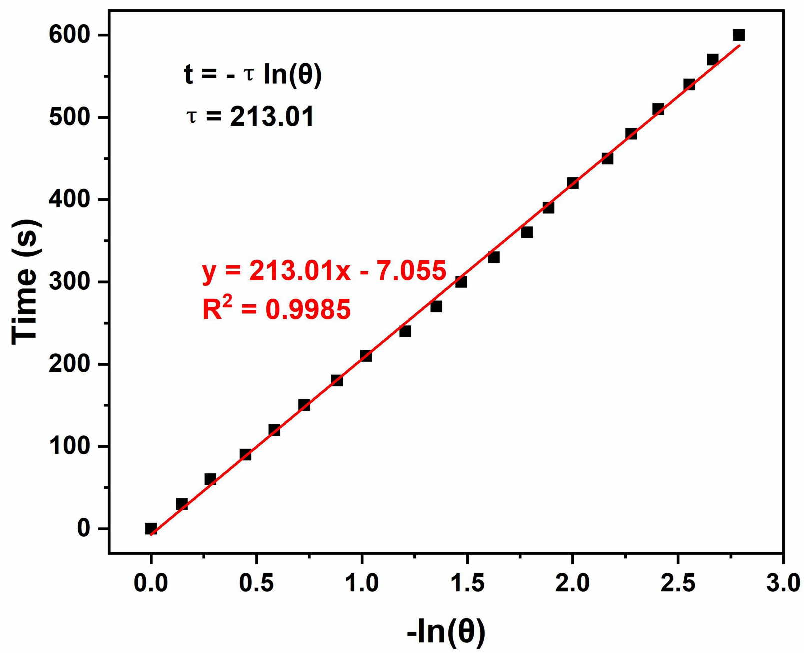

Figure S24. Cooling time versus negative natural logarithm of the temperature obtained from the cooling period.

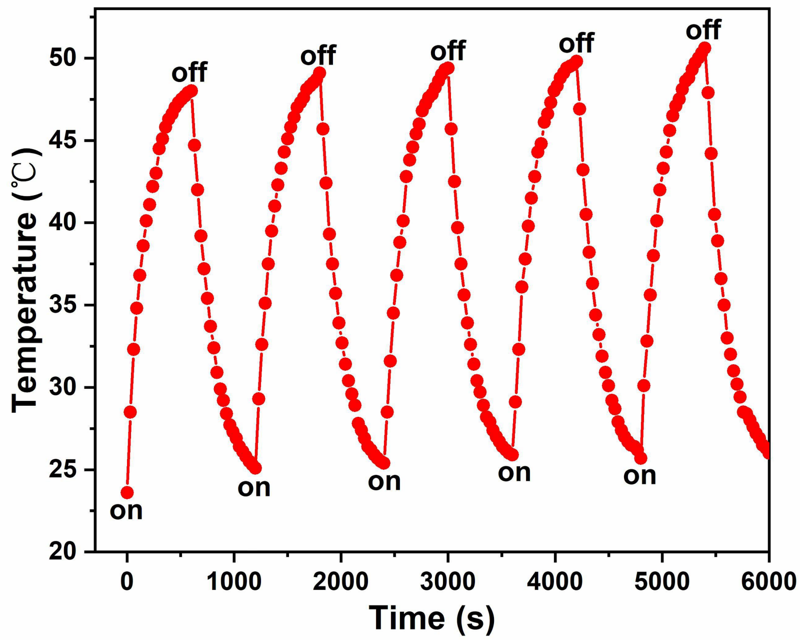

Figure S25. Temperature change of ZnPc 1 for five irradiation/cooling cycles (1.75 W/cm^2).

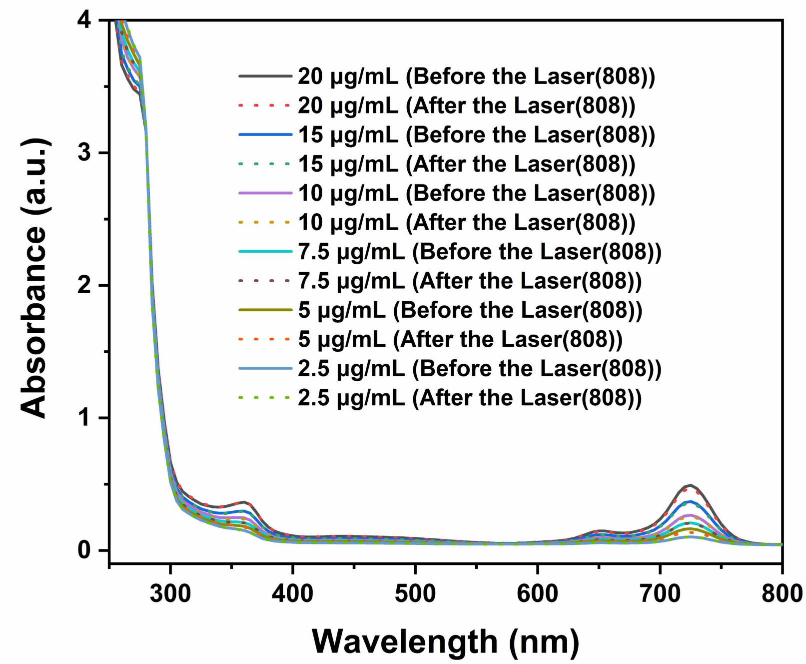

Figure S26. UV–Vis absorption spectra of ZnPc 1 with different diluting factor before and after five irradiation/cooling cycles (808 nm, 1.0 W/cm^2, 10 min).

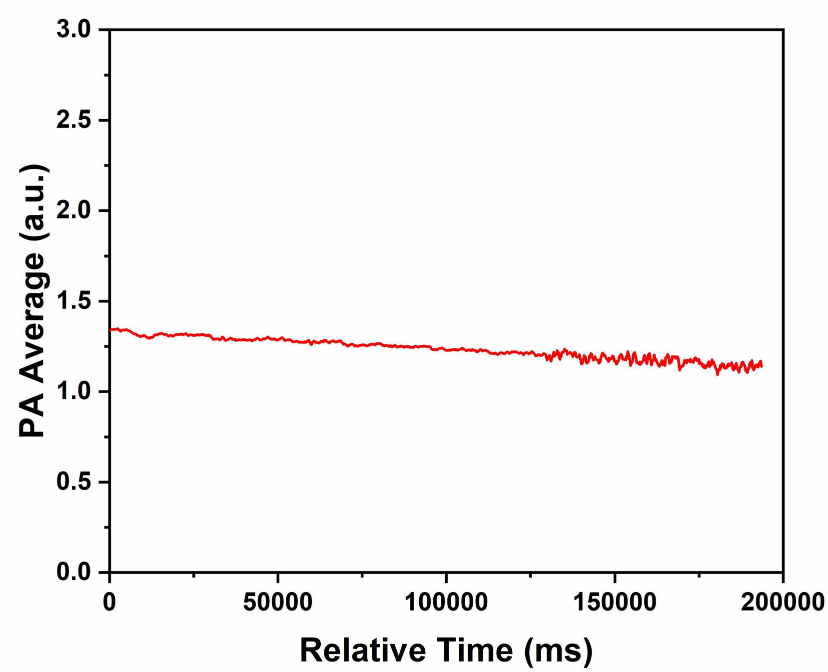

Figure S27. PA stability of ZnPc 1.

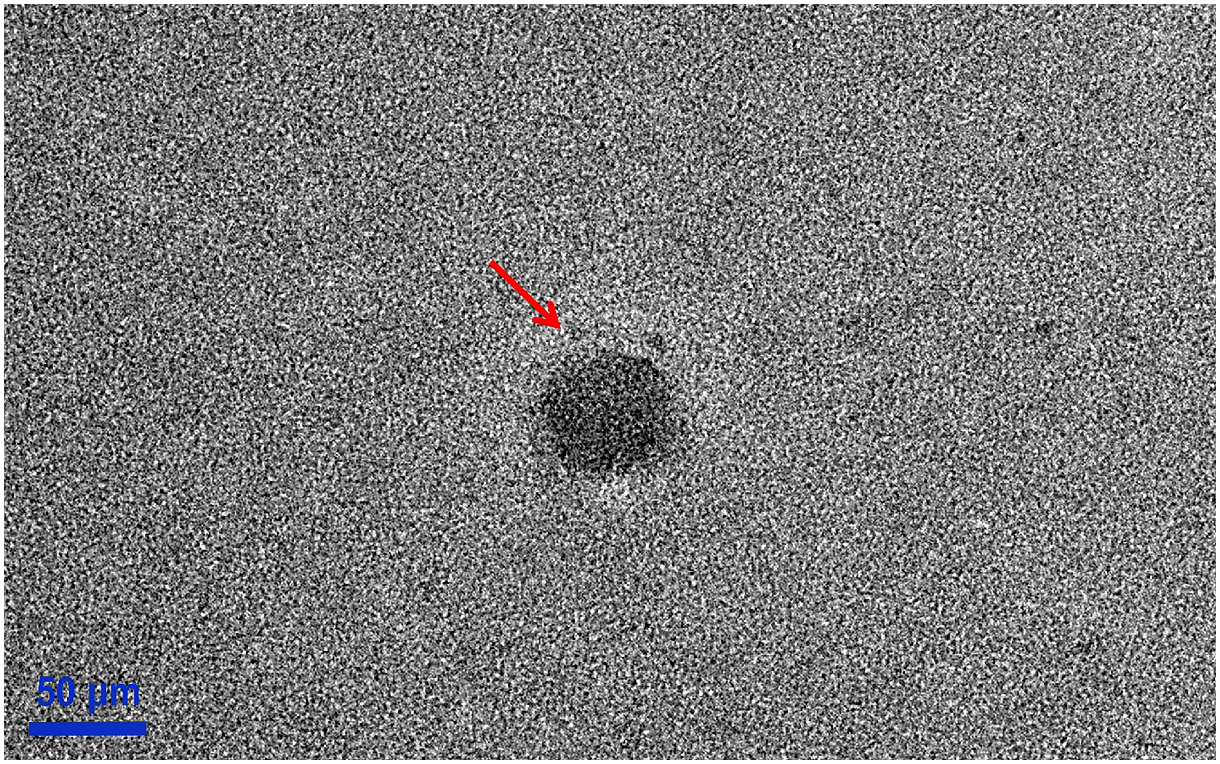

Figure S28. TEM images of ZnPc 1 NPs (The red arrow indicates that ZnPc 1 NPs are spherical nanoparticles).

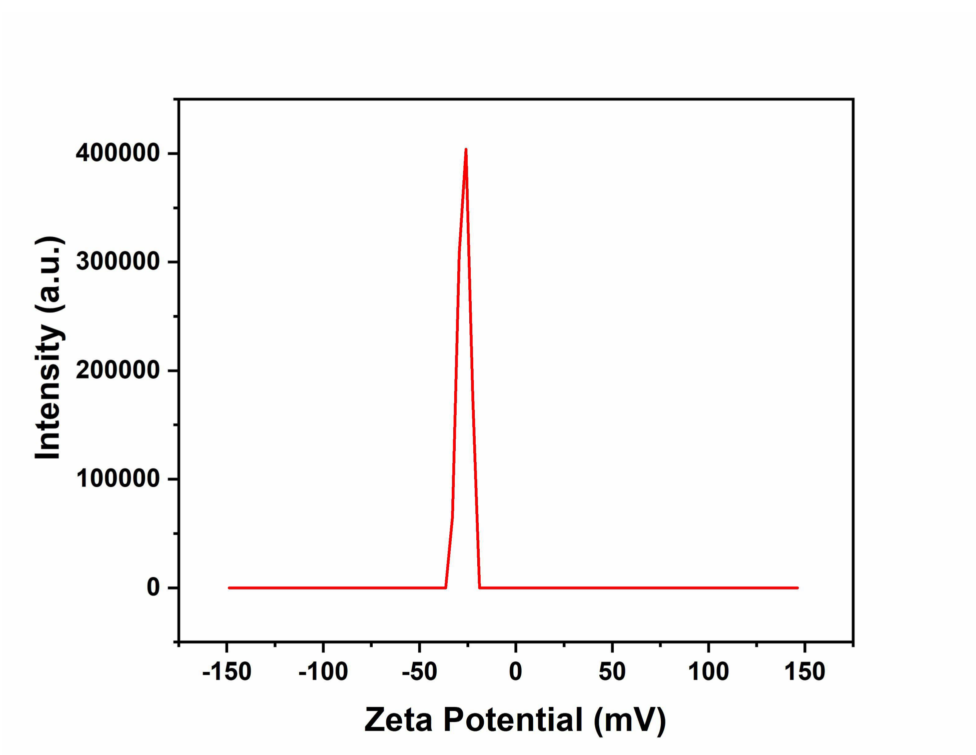

Figure S29. Zeta potentials of ZnPc 1 NPs.

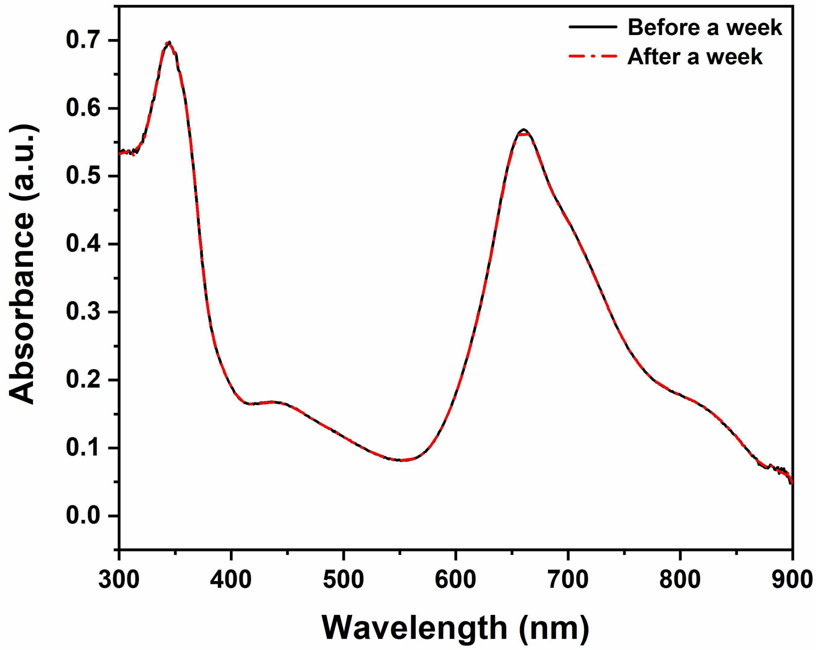

Figure S30. Stability of NPs within a week storage under 4°C.

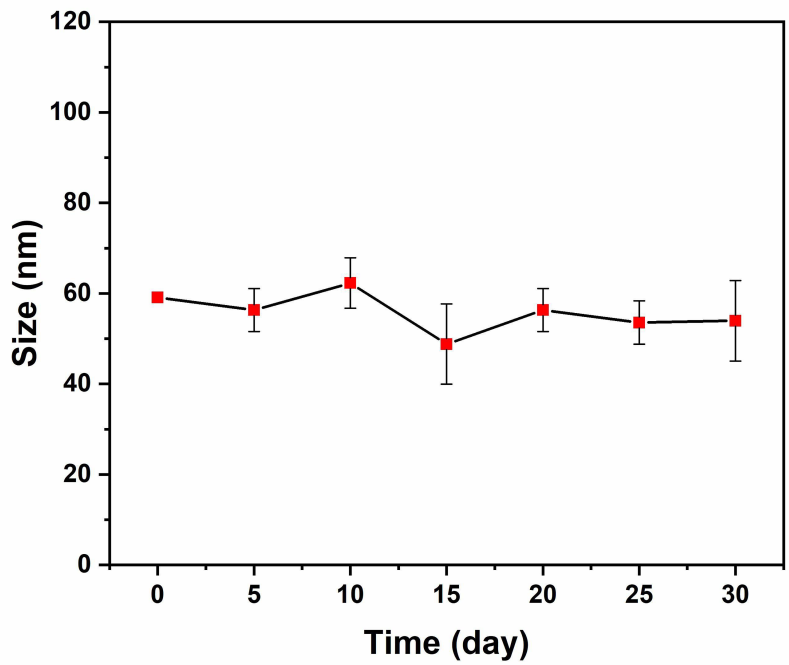

Figure S31. Stability of NPs within a month storage under 4°C.

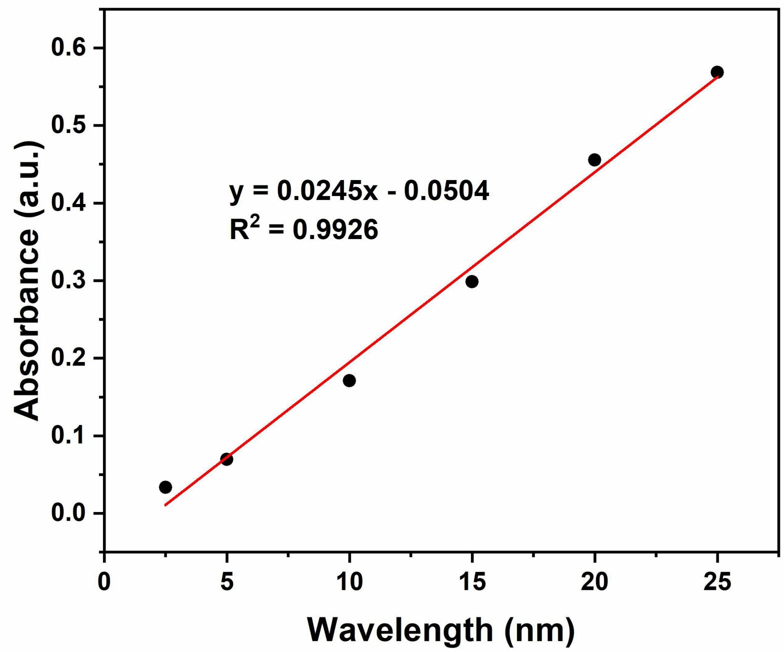

Figure S32. The liner plot of the absorbance of ZnPc 1 NPs in the Q-band (λ max) as a function of concentration.

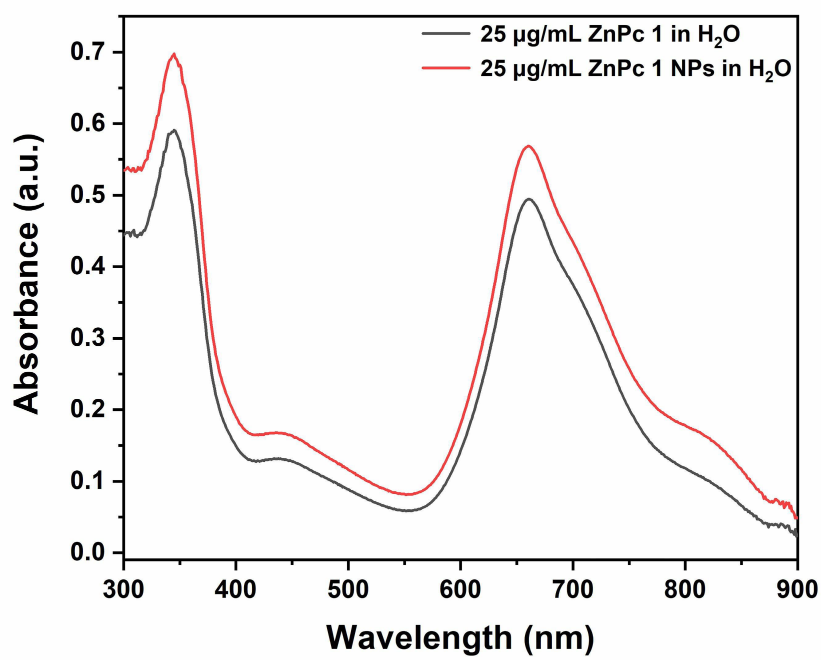

Figure S33. Comparison of UV–Vis absorption spectra of ZnPc1 and ZnPc 1 NPs with the same concentration in water.

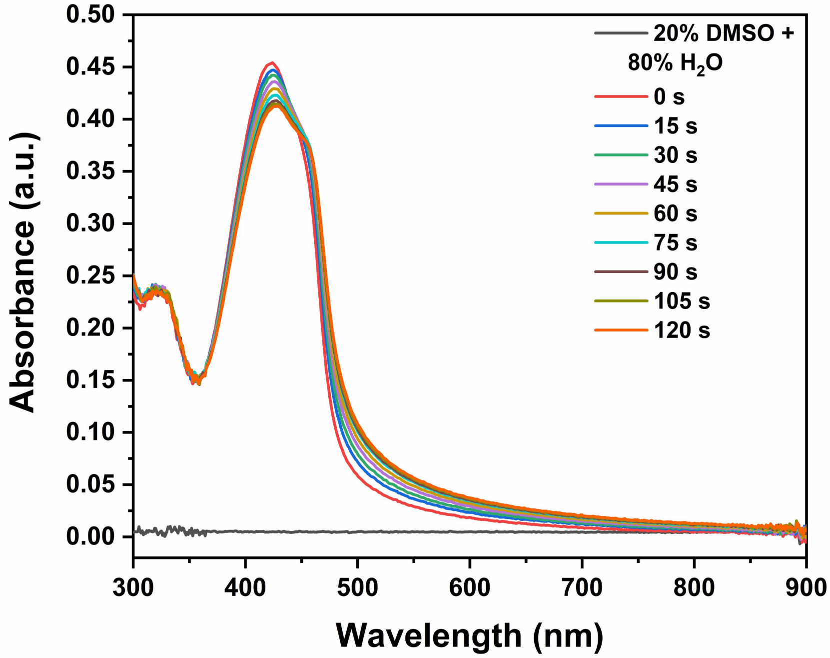

Figure S34. The UV–Vis spectra of DPBF in water containing 20% DMSO for different irradiation times under 690 nm laser irradiation (0.2 W/cm^2).

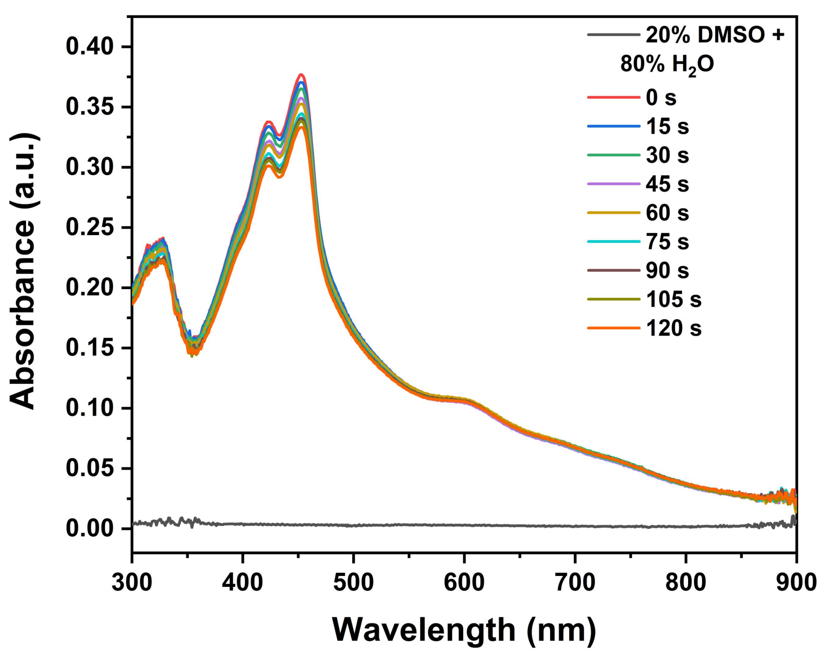

Figure S35. The UV–Vis spectra of DPBF containing ZnPc in water containing 20% DMSO for different irradiation times under 690 nm laser irradiation (0.2 W/cm^2).

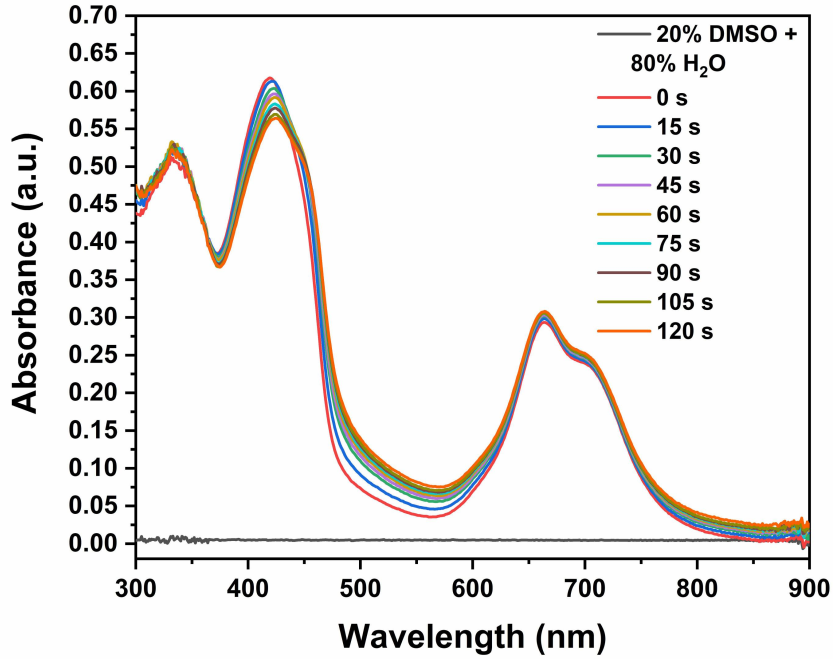

Figure S36. The UV–Vis spectra of DPBF containing ZnPc 1 in water containing 20% DMSO for different irradiation times under 690 nm laser irradiation (0.2 W/cm^2).

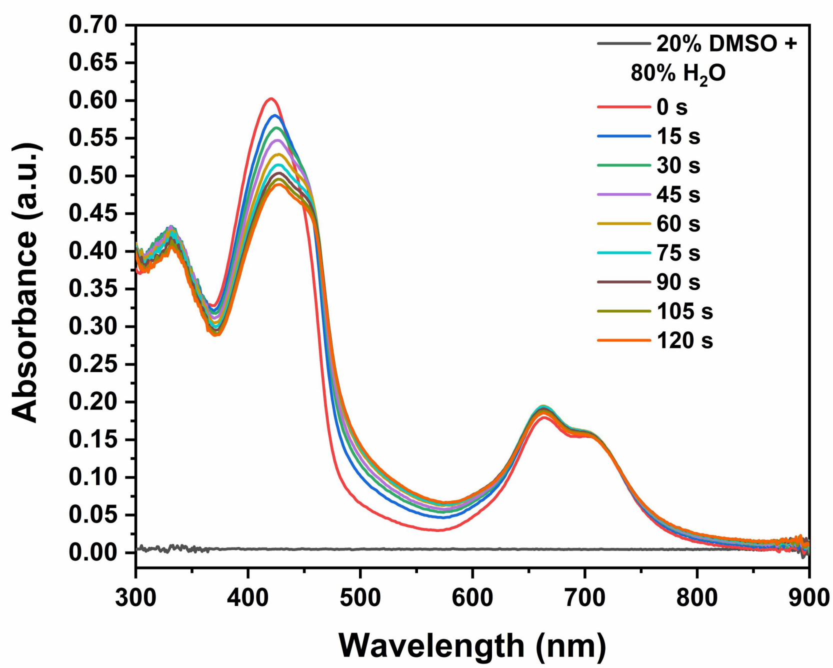

Figure S37. The UV–Vis spectra of DPBF containing ZnPc 1 NPs in water containing 20% DMSO for different irradiation times under 690 nm laser irradiation (0.2 W/cm^2).

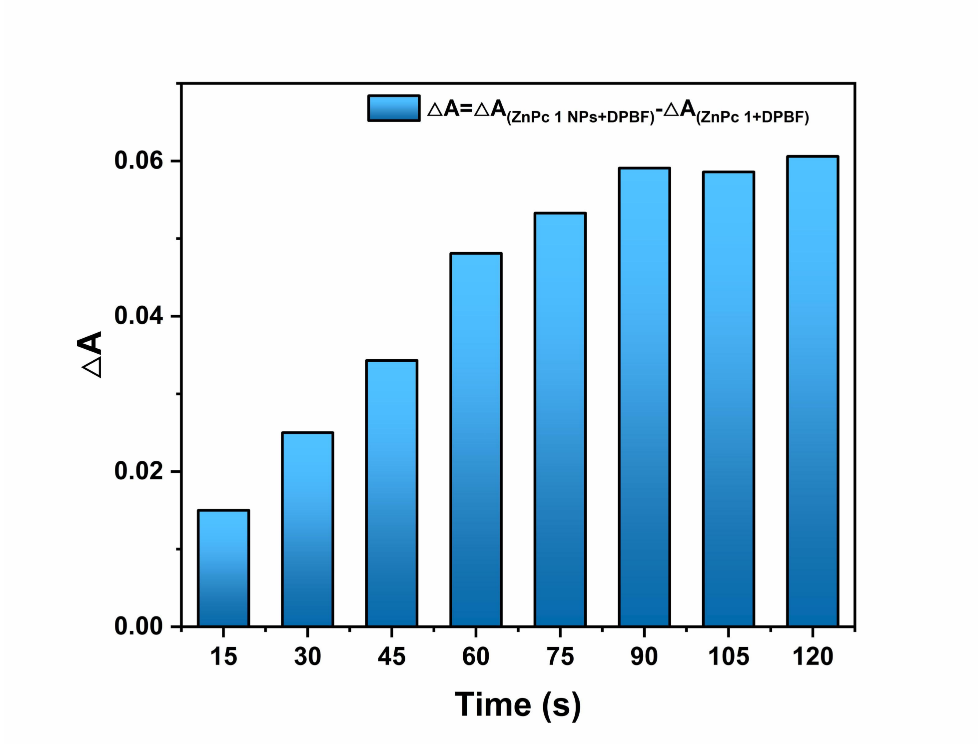

Figure S38. The corresponding relative Increased absorbance variations of ZnPc 1 NPs at different irradiation times under the 690 nm laser irradiation (0.2 W/cm^2).

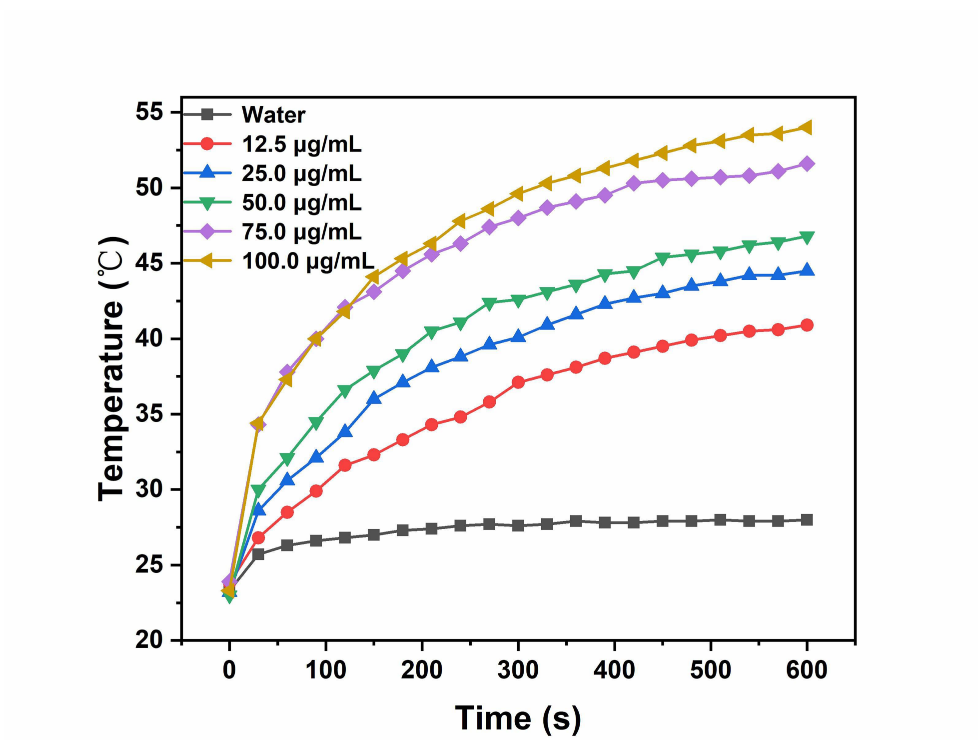

Figure S39. Temperature elevation of ZnPc 1 NPs in dependence of concentration (808 nm, 1.0 W/cm^2).

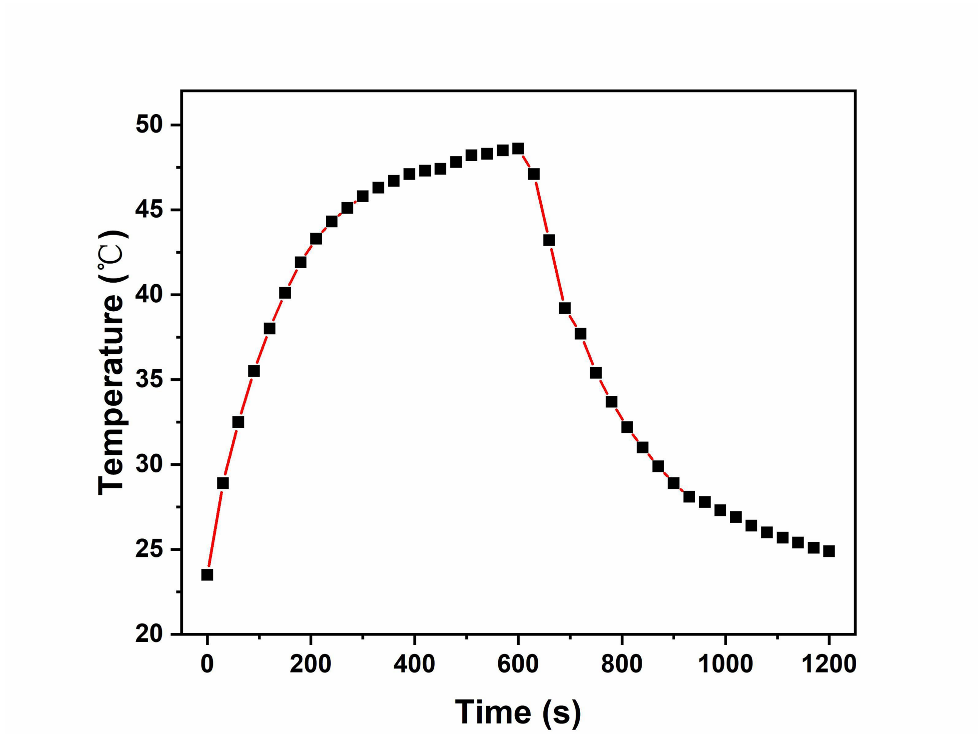

Figure S40. Photothermal effect of ZnPc 1 NPs irradiated with 808 nm laser (1.0 W/cm^2).

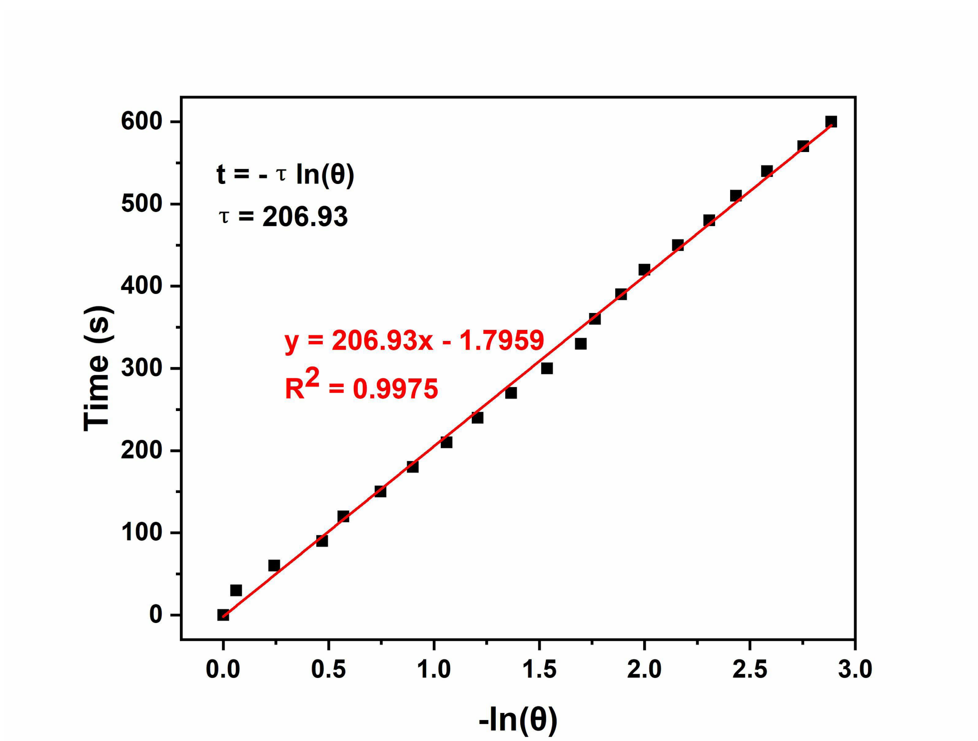

Figure S41. Cooling time versus negative natural logarithm of the temperature obtained from the cooling period.

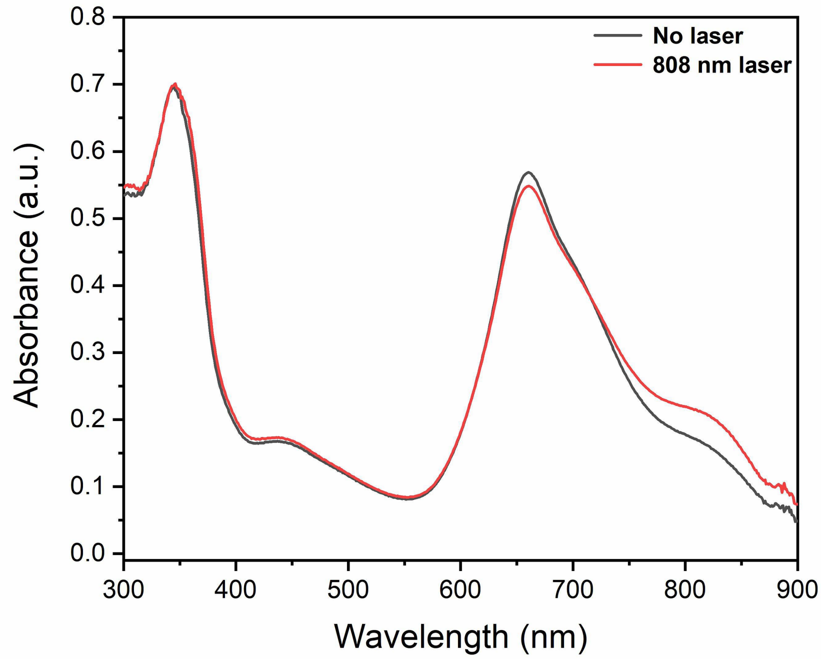

Figure S42. UV–Vis absorption spectra of ZnPc 1 NPs before and after 808 nm laser radiation (1.0 W/cm^2, 10 min).

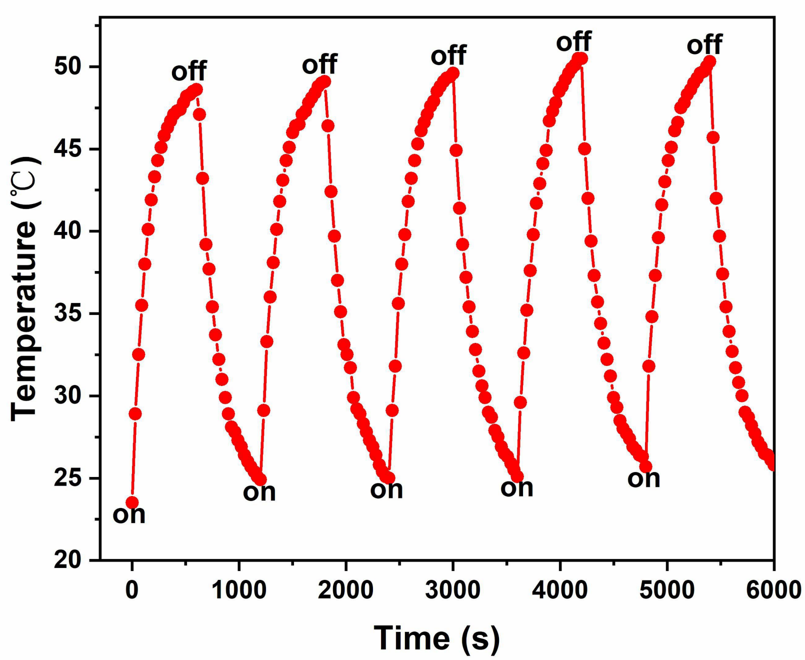

Figure S43. Temperature change of ZnPc 1 NPs for five irradiation/cooling cycles (1.0 W/cm^2).

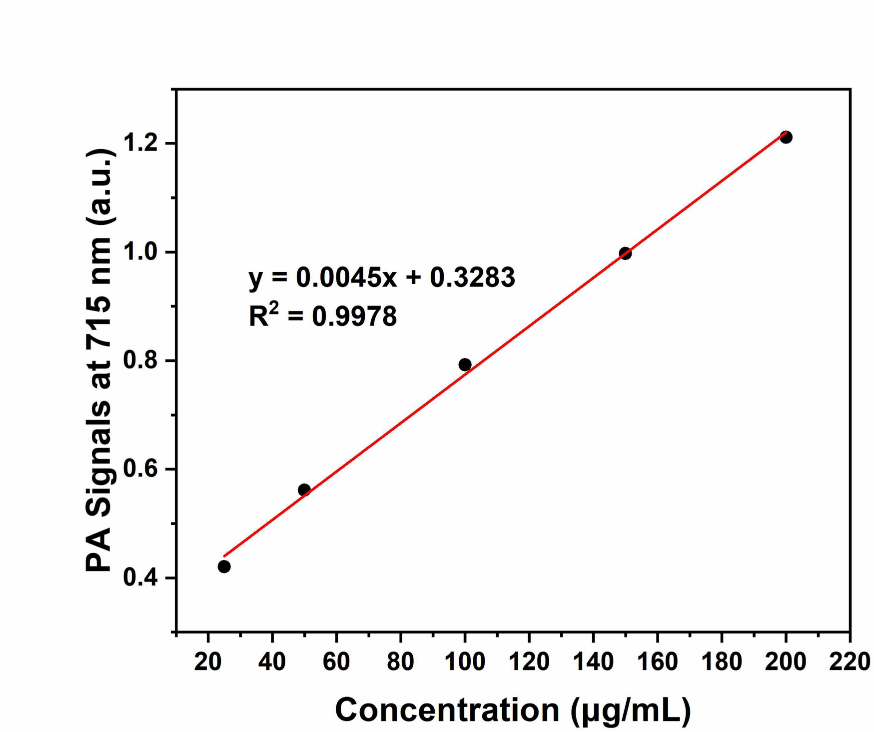

Figure S44. Temperature change of ZnPc 1 NPs for five irradiation/cooling cycles (1.0 W/cm^2).

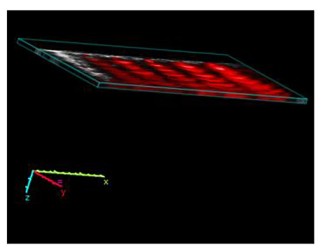

Figure S45. *In vitro* 3D-PA images (no render) of ZnPc 1 NPs upon excitation wavelength at 710 nm at corresponding concentrations.

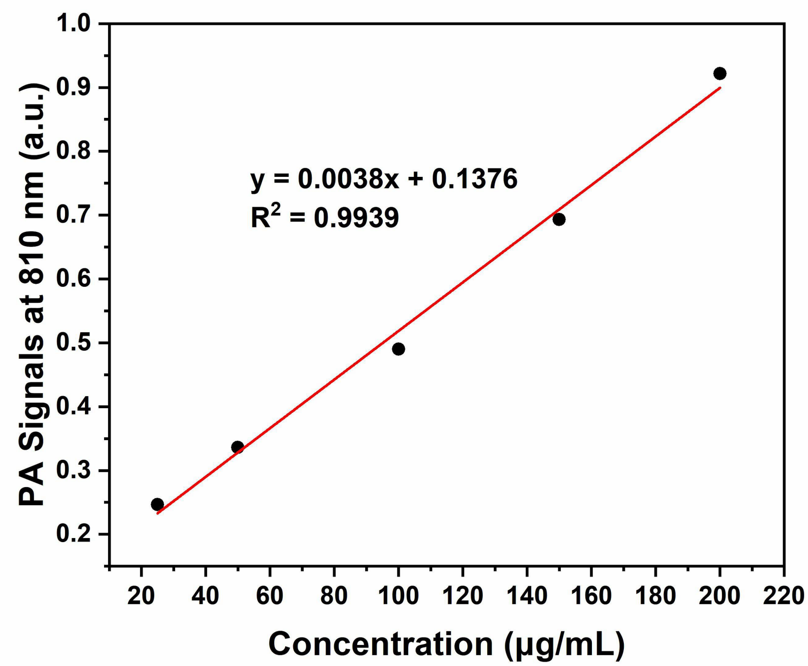

Figure S46. The liner plot of the PA signal of aqueous dispersions of ZnPc 1 NPs at 810 nm as a function of concentration.

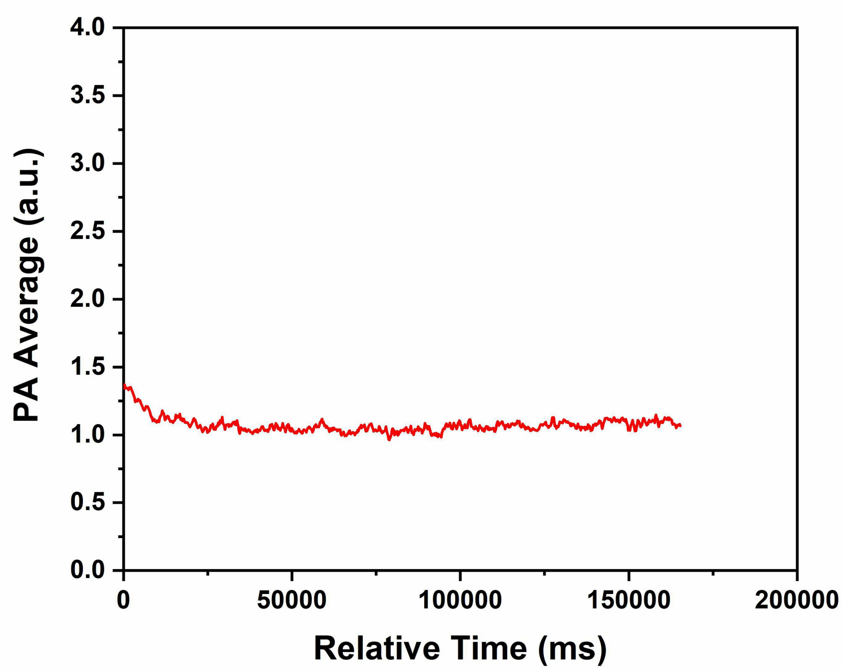

Figure S47. PA stability of ZnPc 1 NPs.

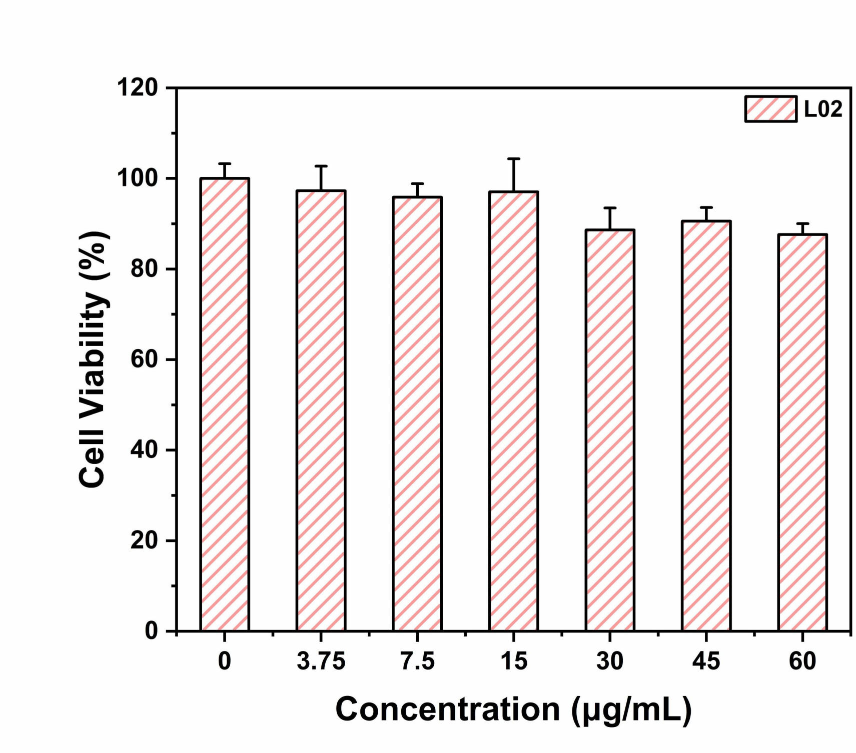

Figure S48. Viability of L02 cells treated with various concentrations of ZnPc 1 NPs in dark. (n=3).

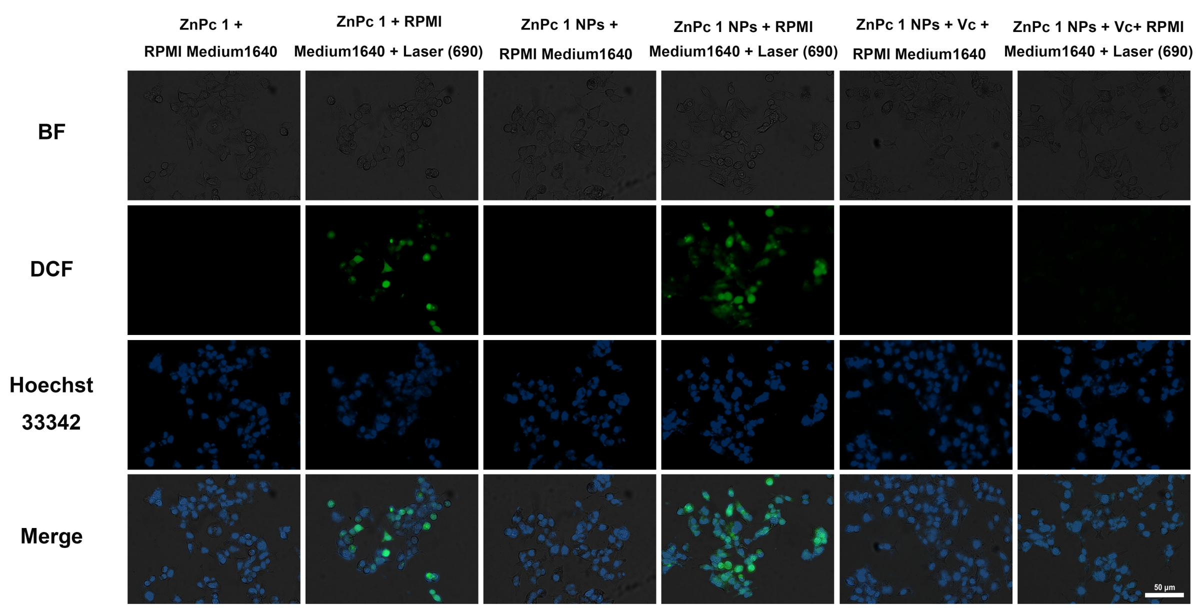

Figure S49. Intracellular generation of ROS in HepG2 cells after different treatments with CM-H2DCFDA as a probe. (Scale bar represents 50 µm.)

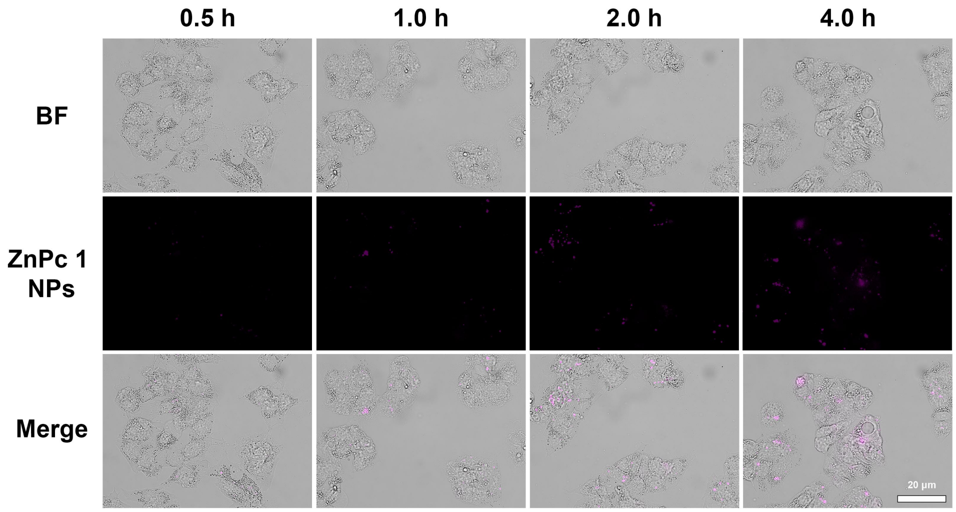

Figure S50. Cell uptake of ZnPc 1 NPs at different incubation times on HepG2.

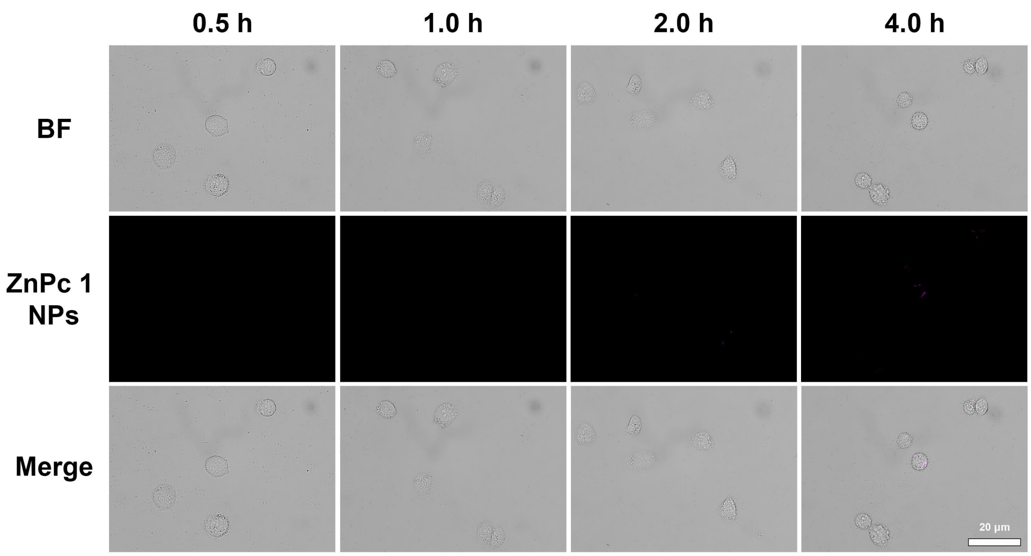

Figure S51. Cell uptake of ZnPc 1 NPs at different incubation times on L02.

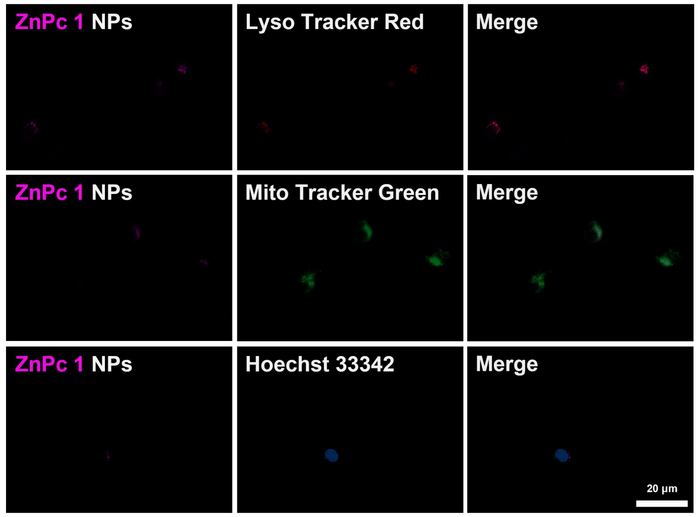

Figure S52. Confocal fluorescence images of L02 cells stained with LysoTracker Red, Mito Tracker Green and Hoechst 33342 following incubation with ZnPc 1 NPs for 4 h. (Scale bar represents 20 μm.)

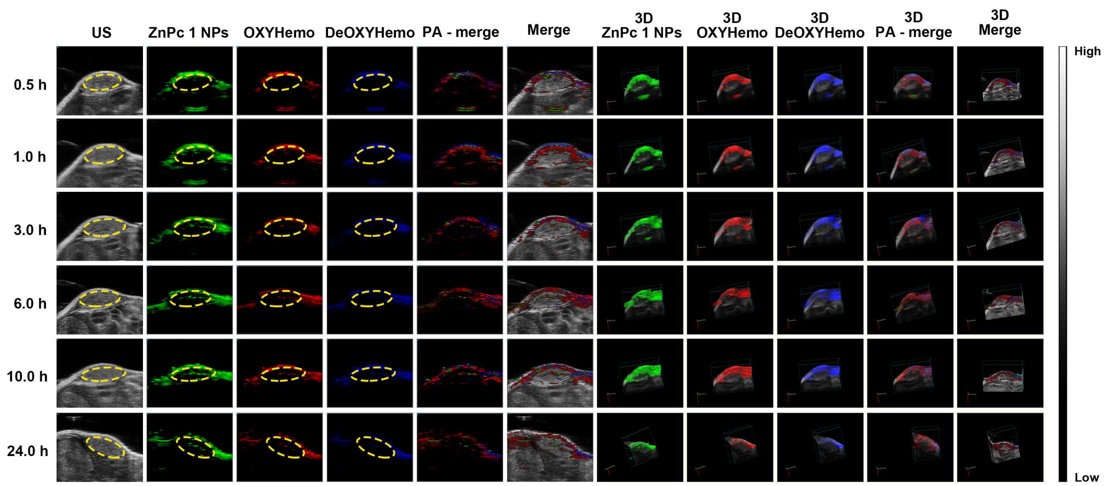

Figure S53. PA images of tumor site at different time points (0.5, 1, 3, 6, 24 h) after intravenous injection of ZnPc 1 NPs (100 μg/mL, 100 μL). (These colored circles represent the location of the tumor.)

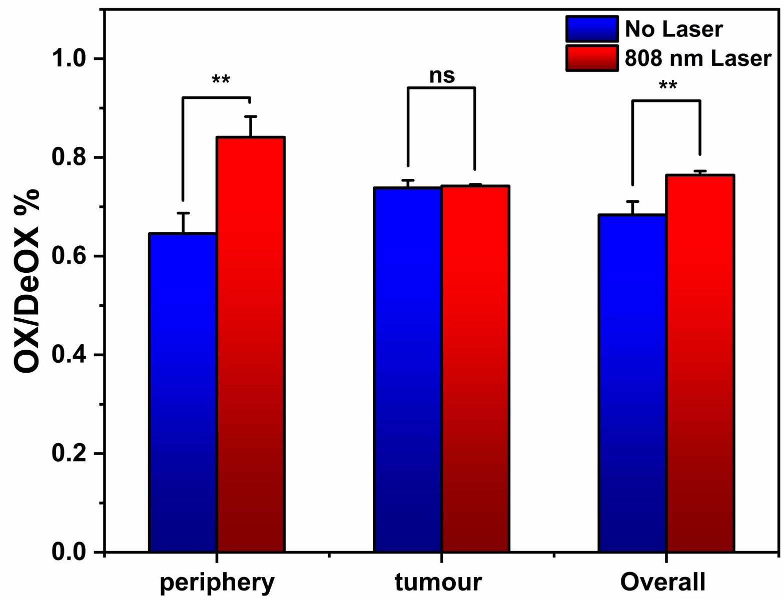

Figure S54. Comparison of oxygen signal/ hypoxia signal (OX/DeOX) in tumor, para-tumor site and the overall at before and after 808 nm irradiation with PA mode. (The dual star indicators indicate a significant statistical difference in OX/DeOX% before and after Laser (808) illumination, whether in the eriphery or overall). Data are presented as mean ± SD ($n = 3$;**$p < 0.01$). **Abbreviation**: ns, not significant.

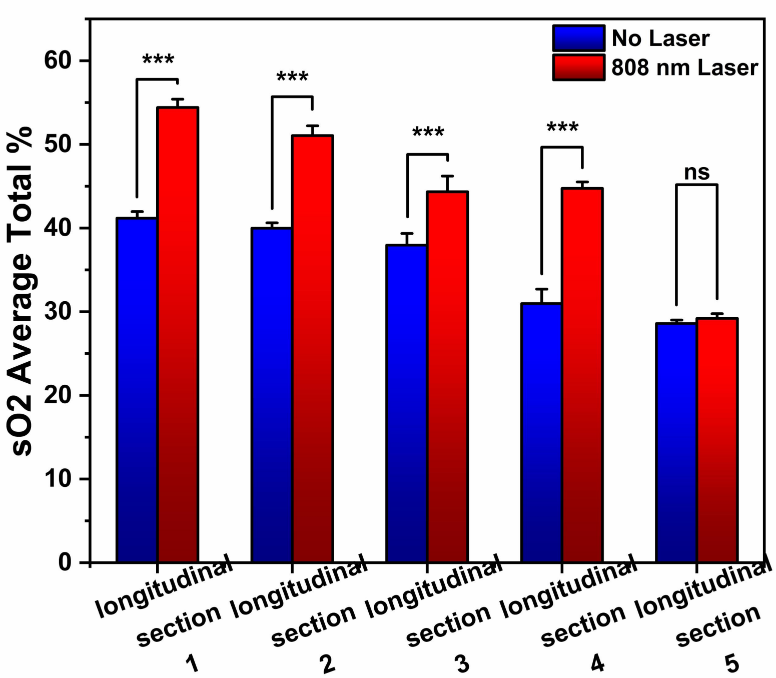

Figure S55. Comparison of the blood oxygen signal (sO2 Average Total) of the scanning sections at para-tumor site under before and after 808 nm irradiation with PA probe under OXYHemo mode. (The triple asterisk indicators indicate an extremely significant statistical difference the blood oxygen signal (sO2 Average Total) of the scanning sections (from section 1 to section 4) at para-tumor site under before and after 808 nm irradiation). Data are presented as mean ± SD (n = 3;***p < 0.001). **Abbreviation**: ns, not significant.

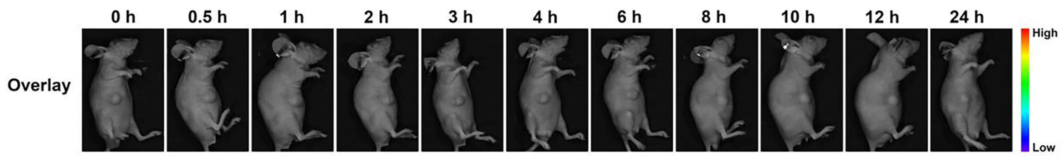

Figure S56. *In vivo* FL images of HepG2 tumor-bearing nude mice at different time points after intravenous injection with PBS.

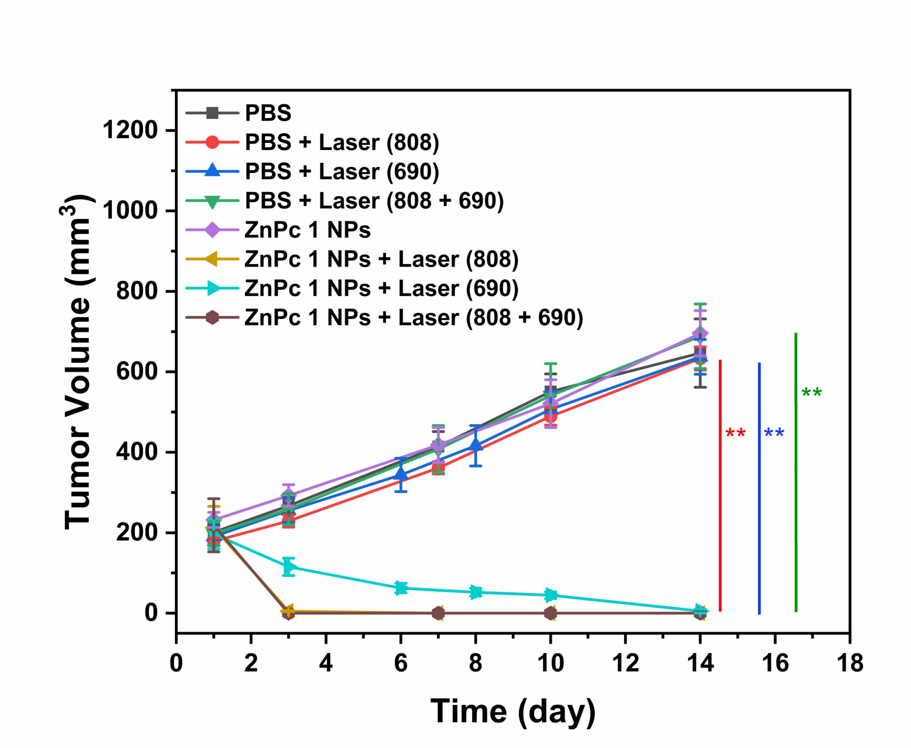

Figure S57. Tumor growth curve and of HepG2-tumor bearing mice after different treatments. (The red asterisk indicators indicate a significant difference between the PBS+Laser (808) group and the ZnPc 1 NPs+Laser (808) group; The blue asterisk indicators indicate a significant difference between the PBS+Laser (690) group and the ZnPc 1 NPs+Laser (690) group; The green asterisk indicators indicate a significant difference between the PBS+Laser (808+690) group and the ZnPc 1 NPs+Laser (808+690) group.) Data are presented as mean ± SD (n = 6;**p < 0.01).

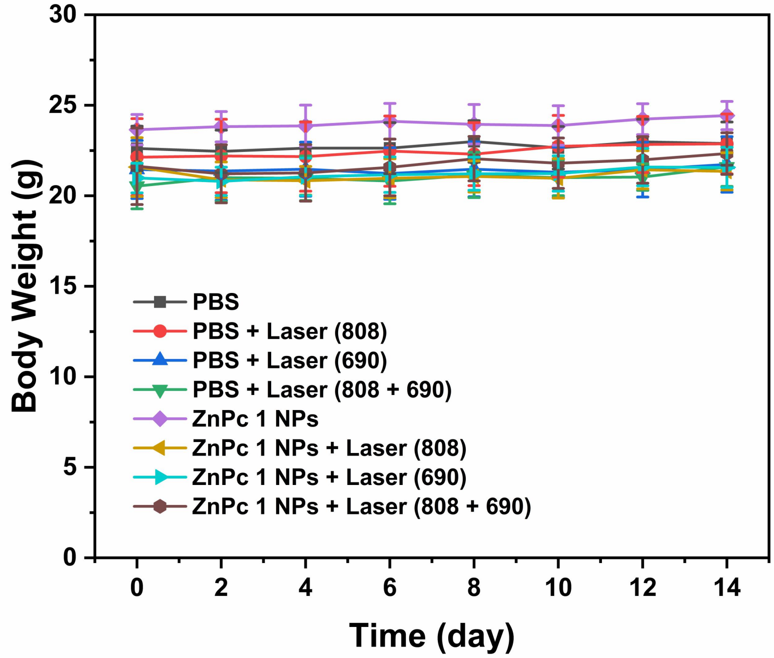

Figure S58. Body weight variation of HepG2-tumor bearing mice after different treatments.

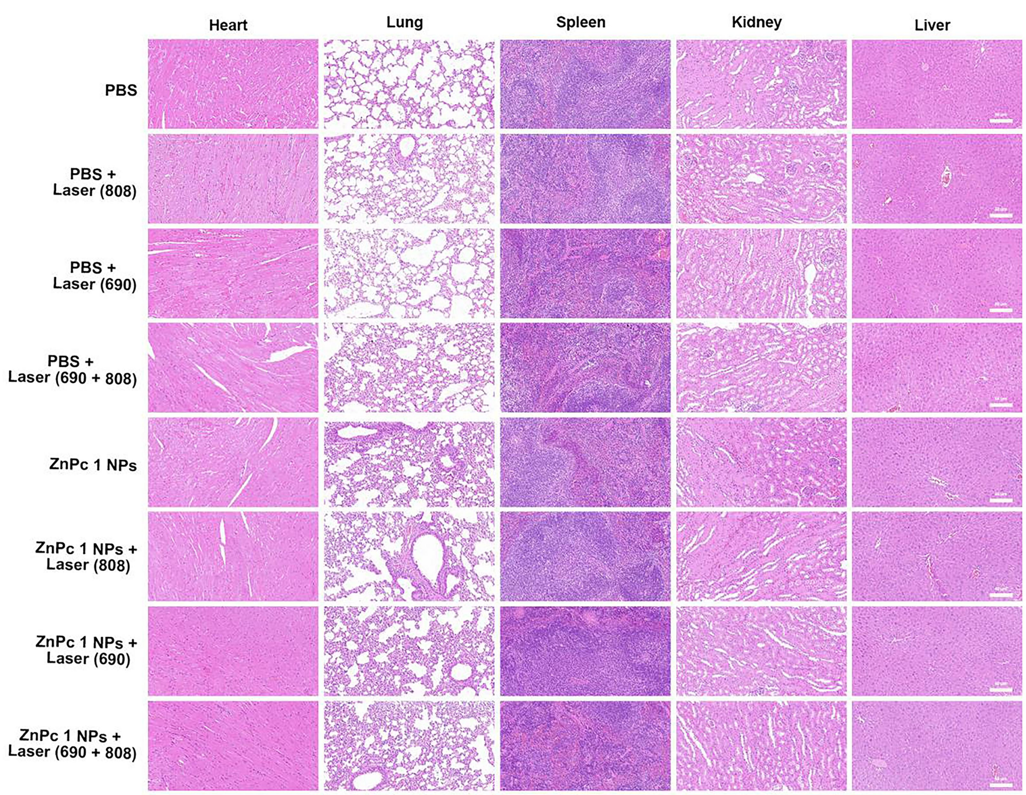

Figure S59. Histological observation of the organs from different treated groups of mice stained with H&E. (Scale bar represents 50 μm.)

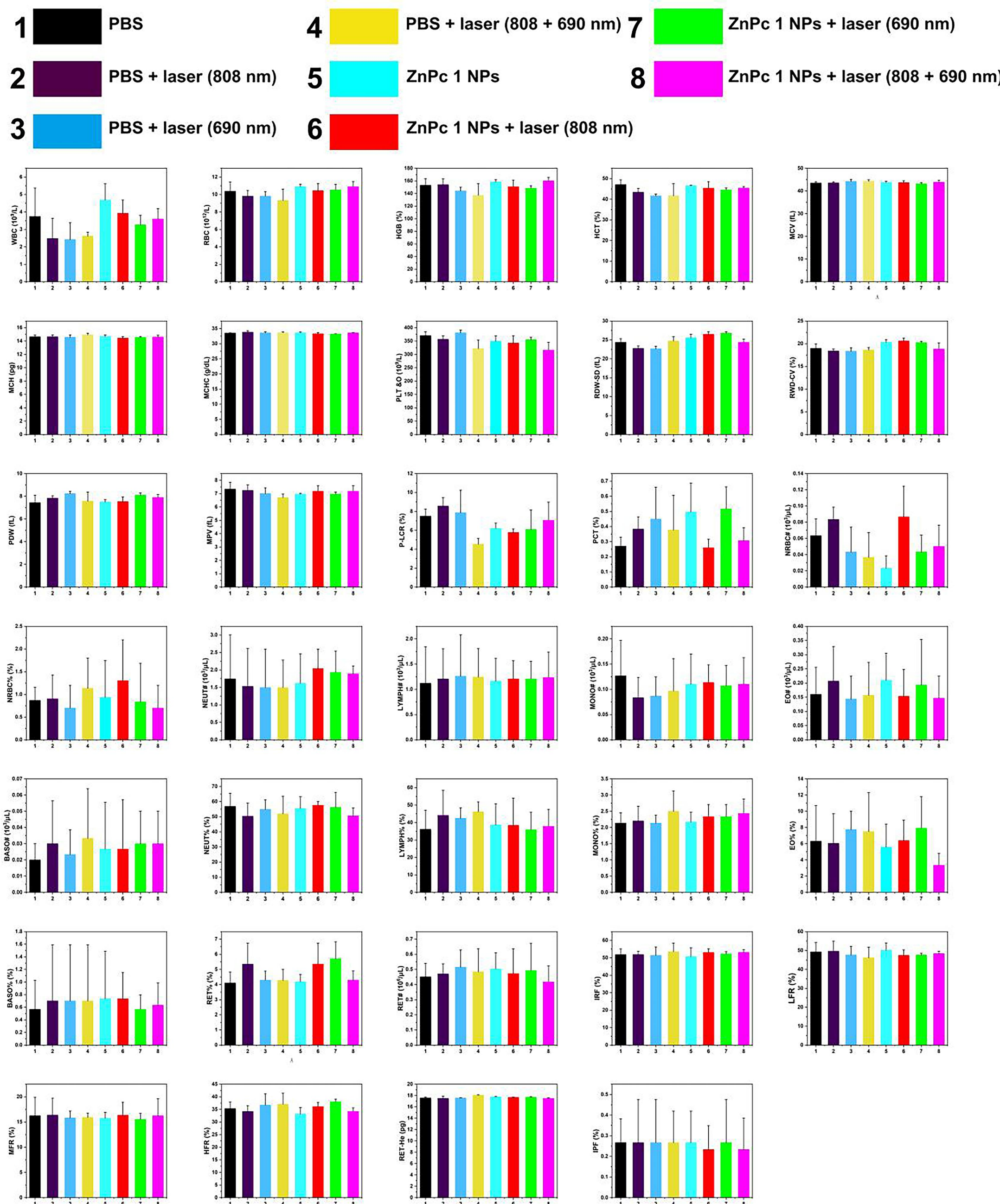

Figure S60. Blood routine examination of the mice with intravenous administration of ZnPc 1 NPs 14 days post-injection under various treatments. (Numbers from 1 to 8 correspond to eight groups of mice as follows: "PBS", "PBS + laser (808 nm)", "PBS + laser (690 nm)", "PBS + laser (808 + 690 nm)", "ZnPc 1 NPs", "ZnPc 1 NPs + laser (808 nm)", "ZnPc 1 NPs + laser (690 nm)" and "ZnPc 1 NPs + laser (808 + 690 nm)", which are marked in different colors, including black, dark-purple, light-blue, yellow, bright-blue, red, green, and pink-purple.)